Flow cytometry for immune characterization in homogenized mouse brain: A systematic review

Robert C. Sharp[1] and Matthew J. Farrer[1*]

[1]McKnight Brain Institute, Department of Neurology, University of Florida, Gainesville, FL., USA[*]

Correspondence:

Matthew J. Farrer

m.farrer@ufl.edu

Keywords: Neuroimmune, Flow Cytometry, Mouse Studies, Immunity, Systematic Review, Inflammation, Neurological Disorders, Methodology.

Main Text Word Count: 5310

Figures: 7 and Suppl. Figures: 3

Tables: 1 and Suppl. Tables: 3

Abstract

Objective: To systematically review the neuroimmunology literature to determine the average immune cell counts reported by flow cytometry in wild-type (WT) homogenized mouse brain.

Background: Mouse models of gene dysfunction are widely used to study age-associated neurodegenerative disorders, including Alzheimer's disease and Parkinson's disease. The importance of the neuroimmune system in multifactorial disorders has become increasingly evident, and methods to quantify resident and infiltrating immune cells in brain, including flow cytometry, have been applied numerous times. However, there appears to be no consensus on the best approach to perform flow cytometry, to quantify immune cell counts or report them. The development of more standardized methods would accelerate neuroimmune discovery and validation through meta-analyses.

Methods: Examination of the PROSPERO registry confirmed a systematic review of 'neuroimmunology' by 'flow cytometry' has yet to be reported. A protocol for a systematic review was subsequently based on the Preferred Reporting Items for Systematic Reviews and Meta-Analyses (PRISMA) using Studies, Data, Methods and Outcomes (SDMO) criteria. Literature searches were conducted in Google Scholar and PubMed databases. From that search, 870 candidate studies were identified and 417 studies were assessed for eligibility based on formal exclusion criteria.

Results: Out of the 417 studies reviewed, 52 were eligible for inclusion and comparative analysis. Each study assessed immune cell subsets within homogenized mouse brain and used flow cytometry. Nonetheless, there was considerable variability in methods, data analysis, reporting and results. Descriptive statistics are presented on study designs and results, including medians with interquartile ranges (IQRs) and overall means with standard deviations (SD) for specific immune cell counts and their relative proportions, within and between studies.

Conclusion: Experiments to conduct and report flow cytometry data, derived from homogenized mouse brains, would benefit from a more standardized approach. While within study comparisons are valid, variability in methods, counts and proportions of immune cell populations are too broad for meta-analysis. However, inclusion of a minimal protocol with more detailed methods, controls and standards could enable this nascent field to compare results across studies.

1 Introduction

The mouse has been used to model neurological disorders for many decades, whether lesion models (i.e. inducing a stroke in a mouse specimen), using transgenic or more physiologic gene knock-out or mutant knock-in approaches (1–3). Some illustrations of mouse modeling for neurologic and neurodegenerative disorders include work in Alzheimer's disease (AD), Parkinson's disease (PD), Huntington's disease (HD), multiple sclerosis (MS), psychological/intellectual disabilities (i.e. depression or Down's syndrome), traumatic brain injuries (TBI) and prion diseases (1–3). Most of these disorders are multifactorial, with genetic and environmental components, for which the immune system may provide some integration. Consequently, there has been growing interest in neuroimmunology, and not just focused on resident immune cells within the brain, but also on infiltrating peripheral immune cells (4–7). Recent studies of gut microbiota have highlighted nervous and immune communication between the gut and central nervous system (CNS) (8–10). With this resurgence, researchers have employed traditional (i.e. immunofluorescence/histology slide staining and Western blotting) and contemporary methods (i.e. single-cell genomics and single-cell sorting/staining via flow cytometry) to better characterize specific immune cell subsets within the body and brain.

Specifically, brain resident immune cells, including microglia and astrocytes, have been comprehensively examined in many mouse models of neurologic disorders (4–10). However, the characterization of other immune cell subsets in peripheral blood, the CNS, and within the brain (both residential and infiltrated) has yet to be fully described (4–10). These immune cell subsets include, but are not limited to, natural killer cells (NK cells), T cells, and B cells (4–10). However, validation and comparison through meta-analysis might be enabled if researchers utilize more standardized methods and reporting.

Technologic developments for single-cell isolation and analysis, including single-cell RNAseq, mass cytometry (CYTOF), fluorescence-activated cell sorting (FACS) and multi-color flow cytometry derived immunophenotyping, have illuminated a wide variety of scientific fields (11,12). Of these techniques, FACS and flow cytometry immunophenotyping are most frequently used. Reasons include the ease of use in setting up a flow cytometer or sorter for a variety of applications, the sensitivity of the assay, the specificity of the antibodies used, the potential of those antibodies to be used for both flow cytometry and Western blotting for the same target, and the ability to produce qualitative and quantitative data (12,13).

Nevertheless, flow cytometry has its pitfalls as analytic interpretation of the data depends on the user's preference for gating and target choices (13). Experimentally, flow cytometry is also dependent on the fluorophores and cytometers used, and variation between these instruments may result in false positives and negatives. Nevertheless, such issues can be circumvented by providing multiple controls, such as unstained and fluorescence minus one (FMO) controls, more rigorously described methods and standardization of flow cytometry protocols.

FACs and flow cytometry immunophenotyping have been insightful and widely used in basic immunology that other scientific fields, including neurology, have begun to adopt these methods (14–16). However, the use of flow cytometry for detecting cell types within the brain and CNS warrant more standardized protocols and reporting, now that their utility has been demonstrated. Although mouse immune profiles within the brain have been identified by high-dimensional single-cell mapping using techniques like mass cytometry (CYTOF)(17), at the time of writing and despite numerous publications, the expected cell counts and proportions of each immune subset within the brain of a wild type (WT) mouse have not yet been clearly defined by standard FACS and flow cytometry. Consequently, we have performed a systematic review focused on neuroimmunology and

the use of flow cytometry to detect immune cells derived from homogenized mouse brain. In our results, we summarize the number of immune cells overall and estimate the immune subsets that can be detected via flow cytometry immunophenotyping. Our findings demonstrate a critical need for more standardized methods and reporting, and have led to best practice recommendations for future publications.

2 Methods

2.1 Study design

Study design was informed by prior literature (18–20) and based upon the Preferred Reporting Items for Systematic Reviews and Meta-Analyses (PRISMA) criteria (21) and Cochrane Handbook of reporting methodology reviews, employing SDMO (Types of Studies, Types of Data, Types of Methods, and Types of Outcome Measures) criteria (22,23). Bias assessment for each individual study selected for systematic review inclusion was also conducted using Systematic Review Centre for Laboratory animal Experimentation (SYRCLE) (24) methodology, and subsequent reporting uses the *robvis* R package and Shiny web app (25).

2.2 Search strategy

Google Scholar and PubMed databases were used to identify all studies for this systematic review, published between Jan 2013 and May 2023. The search protocol and study design were also assessed within the National Institute of Health (NIH) PROSPERO registry database, which confirmed a review of this topic has not been previously conducted. For database searches, the following combination of keywords were used to identify eligible studies: “flow cytometry” AND “immune subset name examined in study” AND “mouse brain.” For example, a keyword search containing “flow cytometry, CD4 T cells, mouse brain”. “Immune subset name examined in study” is defined as

one of the following immune cell subsets: “S100B Astrocytes,” “GFAP Astrocytes,” “GFAP S100B Astrocytes,” “CD4 T cells,” “CD8 T cells,” “double negative DN T cells,” “regulatory T cells TREG,” “follicular helper T cells TFH,” “T helper 1 T cells TH1,” “T helper 2 T cells TH2,” “T helper 17 T cells TH17,” “naïve T cells,” “naïve CD4 T cells,” “naïve CD8 T cells,” “naïve-like T cells,” “central memory T cells TCM,” “central memory CD4 T cells TCM,” “central memory CD8 T cells TCM,” “effector memory T cells TEM,” “effector memory CD4 T cells TEM,” “ effector memory CD8 T cells TEM,” “effector memory T cells re-expressing CD45RA TEMRA,” “effector memory CD4 T cells re-expressing CD45RA TEMRA,” “effector memory CD8 T cells re-expressing CD45RA TEMRA,” “natural killer cells NK cells,” “dendritic cells DC,” “B cells,” “monocytes,” “macrophages,” “M1 macrophages,” “M2 macrophages,” “TMEM119 microglia,” “TMEM119 IBA1 microglia,” or “IBA1 microglia.”

2.3 Selection and exclusion criteria

Studies were selected from search results employing the following inclusion criteria: 1) any study performed between 2013-2023; 2) any study that contained flow cytometry data identifying immune cell subsets and counts in mouse brain; 3) any study that reported total cell numbers or total live cell percentages for one or more immune cell subsets, and; 4) any study that had WT mice or a non-treated control (when reporting on transgenic mouse models). Studies were excluded from search results based upon the following criteria: 1) studies performed in 2012 and prior; 2) any study not focused on flow cytometry of homogenized mouse brains; 3) rat studies; 4) human studies, or; 5) studies not reporting controls or the background mouse strain.

2.4 Data extraction

For each study, information on the mouse strain used, age, and gender were recorded. In addition, methodological information on mouse perfusion, brain extraction and homogenization were recorded.

Flow cytometry methods were recorded when the following was reported: 1) cytometer make and model; 2) software for data collection/analysis; 3) full gating strategy; 4) total cells collected per sample; 5) total live cell counts; 6) total immune cell subset percentages calculated directly from live cell counts, and; 7) methods for determining cell counts and/or mean fluorescence intensity (MFI) readings.

Studies were subsequently examined for immune cell subset counts from WT/control mouse brains directly from the main text, supplementary materials, and/or extrapolated from the figures and graphs presented. In this systematic review, "raw" total immune cell subset counts were reported for each immune cell subset as a median with an interquartile range (IQR; defined as: 75th percentile upper quartile [Q3] – 25th percentile lower quartile [Q1]) and as the combined mean with standard deviation (SD) of multiple studies (n). The "raw" total overall cell count collected per sample by flow cytometry was also reported from these studies.

2.5 Data analysis

After the median with IQR and combined means with SD from the "raw" total immune cell subset counts and from the "raw" total overall cell count collected per sample were recorded from each study, we standardized an approach to estimate how many immune cells of each subset would be counted if the total homogenized mouse brain cells collected by flow cytometry equaled a total of 1×10^5 collected cells. The value of cells required, per sample, for an accurate flow cytometry reading is stated to be between 1×10^4 total cells (minimum) and 1×10^6 total cells (maximum) hence we used the median (26).

Standardized total cell counts for each immune cell subset reported in this systematic review, were calculated using the following equation:

$$\frac{a}{b} = \frac{X}{1\ x\ 10^5\ Total\ Cells\ Collected}$$

Where “a” is the [Raw Total Immune Cell Subset Count], “b” is the [Raw Total Cell Count Collected] per sample, where “X” is the [Standardized Total Immune Cell Subset Count]. Rearranging to solve for X gives the following equation:

$$\frac{(a)(1\ x\ 10^5\ Total\ Cells\ Counted)}{b} = X$$

Once all total immune cell subset counts were standardized, we determined the theoretical standardized percentages of each immune cell subset within the entire mouse brain, and report those results as means with SD.

3 Results

3.1 Literature search and selection of studies for review

A PRISMA based flow diagram illustrates our screening methodology for study identification (**Figure 1**) (21). The two databases (Google Scholar and PubMed) searched using the keyword search terms, defined in Methods, highlighted 870 articles for systematic review. Of those 870 reports, 218 were removed as they supplied only an abstract or were duplicated between databases, and 652 studies remained. Of these an additional 235 studies were removed as they were published in 2012 or prior. This cut off is arbitrary, but was used to identify more contemporary flow cytometry immunophenotyping publications and resulted in 417 eligible studies. Further inclusion and exclusion criteria removed: 128 studies in which flow cytometry of homogenized mouse brains was not a main focus; 126 studies with insufficient information and/or results from controls or in which the background mice strain was not specified; 91 human studies, and; 20 rat studies. Consequently,

52 studies that passed our inclusion and exclusion criteria were incorporated in this systematic review (27–78).

3.2 Reporting of mouse information and perfusion/tissue processing is inconsistent between studies.

Of the 52 studies selected, we reviewed the basic characteristics of the mice strains used (**Figure 2A**, **Suppl. Table 1**). The inbred congenic C57BL/6 mouse line was used most (22/52 studies [42.3%]) as a control and as the background for genetically modified mice (29,30,32,33,38,43–49,51,56,60,68–71,74,76,78). Nevertheless, in many studies the nomenclature of this mouse line was inconsistently labeled and often imprecise. Terminology included mention of: C57BL/6J (15/52 studies [28.8%]) (31,34,35,41,54,58,62,64–67,72,73,75); C57/BL6 (2/52 studies [3.84%]) (36,42); C57BL/6 (H-2b) (2/52 studies [3.84%]) (37,55); and C57BL/6J (B6) (2/52 studies [3.84%]) (40,63). . The majority of studies that reported mouse gender (**Figure 2B, Suppl. Table 1**) used only male mice (27/52 studies [51.9%]) (27,31,32,35,36,40,42,43,46,47,49,51,52,56,60–65,67,69–73,76), although 10/52 studies [19.2%] reported mixed results of male and female animals together (29,33,34,38,39,41,45,53,74,77). The age of the mice (**Figure 2C, Suppl. Table 1**) within studies varied but the majority reported findings at 8-10 week (2-2.5 month) (8/52 studies [15.4%]) (36,53,54,57,60,62,69,73). However, studies characterized animals over a wide range of age, from 1-2-weeks (34,41) and between 3-26 months (76).

Perfusion (**Suppl. Figure 1, Suppl. Table 1**) and brain tissue processing methods (**Figure 3A-C, Suppl. Table 1**) also varied across the 52 studies. A majority of studies (30/52 studies [57.7%], **Suppl. Figure 1, Suppl. Table 1**) used cold PBS for perfusion (31,33–35,37,41,45–50,52,54–60,63,65–69,72,75,76,78). Of the 52 studies reviewed, 8/52 [15.4%] (**Figure 3A, Suppl. Table 1**) used a commercial kit, such as the Neural Tissue Dissociation Kit P (Miltenyi Biotec), to isolate

immune cells from mouse brain (27,28,36,42,43,63,69,73). Nevertheless, in neurology it remains unclear how to best process mouse brain to dissociate the tissue and leave cell types intact (79–81). Researchers may use mechanical homogenization, enzymatic homogenization, or both homogenization techniques (79–81). For the studies reviewed, 17/52 [32.7%] (**Suppl. Table 1**) used some type of mechanical homogenization (i.e. Glass-Teflon homogenizer, an 18-gauge needle, etc.) before filtering through a cell strainer, prior to enzyme treatment and the use of a myelin removal gradient (i.e. Percoll gradient) (27,33,35,39,46,50,52,55,57–59,61,62,65,66,68,71). The enzymatic solutions used in the reports were also vary widely (**Figure 3B, Suppl. Table 1**). Most studies used collagenase (I, II, IV, D, or I-S) alone or combined with additional enzymes (20/52 studies [38.5%]) (29–33,35,48,49,56,62,64–66,68–70,72,76–78). The enzyme most used in combination with collagenase (or another tissue digestion enzyme) was DNase I (16/52 studies [30.8%]) (27,29–33,49,50,53,55,56,62,64,65,68,70,72,76–78). After homogenization of mouse brain, cell strainers are generally used to remove dead cells and myelin (**Figure 3A, Suppl. Table 1**), and a 70 μm filter was used in the majority (20/52 studies [38.5%]) of studies (15,29,32,34,35,40,41,45,47,48,50,54,55,58,61,65,66,69,74,76). To further remove myelin from mouse brain homogenate, researchers employ a myelin removal kit or Percoll gradient solutions. Specific cell types can be isolated while the myelin layer rises to the top of the sample tube with centrifuge, depending upon the percentage of Percoll. Again, in the studies reviewed, the percentages of Percoll (**Figure 3C, Suppl. Table 1**) varied with most using a 30%/70% Percoll gradient solution (13/52 studies [25.0%]) (15,29,31,35,45,47,55,59,64,65,73,74,76). Overall, the age of mice and methodology for isolating immune cell counts from brain for flow cytometry varied greatly between studies.

3.3 Flow cytometry methodology used and cell counts are inconsistently reported between studies

After considering mice strain and brain homogenization methods, we examined the flow cytometry instruments used and data reporting (**Figure 4A-C, Suppl. Figures 2A-B and 3A-B, Suppl. Table 2**). The make and model of flow cytometer/FACS sorter (**Suppl. Figure 2A, Suppl. Table 2**) and analysis software (**Suppl. Figure 2B, Suppl. Table 2**) used in each of studies also varied widely. The flow cytometer most reported was the BD LSRII Flow Cytometer (12/52 studies [23.1%]) (32,34,35,37,38,41,45,53,62,63,65,67) whereas the FACS sorter was the BD FACS Aria III (7/52 studies [13.5%])(32,39,48,50,55,56,65). The analysis software most generally used was a version of FlowJo (Tree Star) for flow cytometry immunophenotyping (32/52 studies [61.5%]) (29,31–33,35–38,40,43,45,46,49,51–56,58,60,64,65,67,70–76,78) and BD FACSDiva specifically for FACS analysis (11/52 studies [21.2%]) (27,28,34,37,39,41,44,62–64,78).

After reviewing methodology in all 52 studies, we assessed the quality of flow cytometry reporting (**Figure 4A-C, Suppl. Figure 3A-B, Suppl. Table 2**). For each study, we scored the following parameters: 1) whether a full gating strategy was reported; 2) the total cells collected per sample for flow cytometry; 3) the total live cell counts during flow cytometry sample collection; 4) if the total immune cell subset percentage was calculated directly from the live cell count reported or was it derived from another gate (i.e. was the immune cell subset percentage reported derived from the $CD45^+$ gate or from the live/dead gate); and 5) whether the methods used to determine cell counts and/or MFI readings were documented. Of the 52 studies reviewed, 31/52 [59.6%] included a full gating strategy (**Figure 4A, Suppl. Table 2**) (27–29,32,34–36,38,39,43,45–47,49,52,53,56,57,60,62–66,69,73–78) , while 18/52 [35.6%] reported a partial gating strategy (30,31,37,40,42,44,48,50,51,54,55,58,59,61,68,70–72) and 3/52 [5.8%] of studies did not include this information (33,41,67). On reporting total cells collected per sample during flow cytometry collection (**Figure 4B, Suppl. Table 2**), only 17/52 [32.7%] of studies provided this data (27,28,32,38,39,43,46,49,54,59,60,63,65,69,73,75,76). Total live cell counts collected during flow

cytometry (**Suppl. Figure 3A, Suppl. Table 2**) was only reported in 11/52 [21.2%] of the studies reviewed (27,28,32,39,59,60,63,69,73,75,76). Out of the 52 selected studies, only 14/52 [26.9%] expressed their results in terms of total immune cell subset percentages derived from live cells only (**Figure 4C, Suppl. Table 2**) and not from another gate (such as deriving from the $CD45^+$ gate) (27,28,37,39,45,49,54,60,69,70,73,74,76,78). Lastly, 35/52 [67.3%] of studies (**Suppl. Figure 3B, Suppl. Table 2**) reported methods on how cell counts and/or MFI readings were recorded (27–30,32,34,35,37,39,41,43–46,51–54,56,57,59–61,63–66,69,72–78). Overall, the cytometer/FACS sorter used, and the reporting of total cells collected, total live cells and immune cell subset percentages was not standardized in the 52 studies examined.

3.4 Reported immune cell counts from WT/control homogenized mouse brain is highly variable between studies.

Across all studies we then examined the total immune cell counts reported in WT/control mouse models, as detected by flow cytometry immunophenotyping and/or by FACS (**Suppl. Table 3**). As described in Methods and **Suppl. Table 3**, studies were selected based on their reporting of a wide-variety of immune cell subsets. These included astrocyte subsets, T cell subsets/memory T cells (naïve-like, central memory [T_{CM}], effector memory [T_{EM}] and effector memory re-expressing CD45RA [T_{EMRA}]), natural killer cells (NK cells), dendritic cells (DCs), B cells, monocytes, macrophages (M1 and M2 phenotypes), and different microglia subsets.

Many immune subsets were examined but relatively few were reported in sufficient studies to be able to calculate representative medians with IQR and means with SD (**Figure 5 and Suppl. Table 3**). Immune cell subsets with at least two or more references to derive a median and mean cell count for WT/control mice include: bulk $CD4^+$ T cells (29–35), bulk $CD8^+$ T cells (29,30,32,36–39), double negative (DN) T cells (35,40), regulatory T cells (T_{REG}) (31,41–44), T helper 1 cells (T_{H1}) (29,42), T

helper 17 cells (T_{H17}) (46,47), NK cells (35,43,48,49,51–53), DCs (35,54–57), B cells (35,58–62), monocytes (63–69), bulk macrophages (66,67,70–74), and TMEM119$^+$ IBA1$^-$ "steady state/ramified" microglia (75–78). Immune cell subset counts that were derived from only one study, such as S100B$^+$ only astrocytes (27), GFAP$^+$ only astrocytes (28), follicular T cells (T_{FH}) (45), and T_{EM} bulk CD4$^+$ and bulk CD8$^+$ T cells (32), were still included in this review as a representation of the possible median/average cell count for these subsets.

We first calculated the overall medians for each examined immune subset by collecting all of the "raw" total immune subset cell counts from each of the 52 studies (**Figure 5**). By doing this, we discovered that out of these studies, there were some that were outliers (outside of the IQR) that appear to heavily altered the overall total immune cell counts determined by flow cytometry (29,35,38,43,49,55,60,63,71,74,78). Out of all the immune cell subsets from the 52 studies, the highest median was TMEM119$^+$ IBA1$^-$ "steady state/ramified" microglia (72,300 [IQR=194,038]; n = 4 studies) (75–78). The lowest median that was calculated was T_{FH} T cells (8 [IQR=0]; n = 1 study) (45). Memory T cell subsets found within both CD4$^+$ and CD8$^+$ T cells were not reported as an immune cell subset in any study. Similarly, T helper 2 cells (T_{H2}) were not reported in any studies. It was also surprising that there were no reports on M1 and M2 macrophage counts within mouse brain.

For each of the combined means of the total immune cell subsets found within mouse brains, the 52 studies had a highly variable range, where most of the SD calculated were greater than the calculated means (**Suppl. Table 3**). As with the calculated medians, the highest mean cell count reported from the 52 studies was TMEM119$^+$ IBA1$^-$ "steady state/ramified" microglia (90,323 ± 104,555; n = 4 studies) (75–78). The lowest mean cell counts reported were for T_{FH} T cells (8 ± 0; n = 1 study) (45). Subsequently, we also calculated the combined means of total overall cell counts, collected per sample, as reported in the 52 studies reviewed (**Suppl. Table 3**). Although not as variable as immune

cell subset counts, the total overall cell counts collected by flow cytometry ranged from 1 x 10^4 to ~3 x 10^6 cells. In some studies, the actual number of cells collected by flow cytometry was not specified (27,28,45–47) but the total cell counts could be extrapolated from data given in the main text, figures, and/or supplementary material. Overall, we conclude the immune cell subset counts collected by flow cytometry immunophenotyping are highly variable between studies, and there is currently insufficient data on specific T cell subsets/memory subsets and M1/M2 macrophage counts within the mouse brain.

3.5 Standardizing mean total immune cell subset counts and percentages within WT/control mouse brain.

Due to the high range of SD values derived from the means of the examined immune cell subsets from each of the 52 studies, we sought to determine a way to better standardize the mean total immune cell subset percentages found from within WT/control mouse brain in each study (**Figure 6, Suppl. Table 3**). Our approach stems from the idea that flow cytometry data that counts individual cell percentages should be reported as values from the total number of cells collected (on average 1 x 10^5 cells) and should not be derived from a sub-partition within the gating strategy (26,82). Thus, based on the assumption the total cells collected per sample was 1 x 10^5 cells, we were able to estimate a standardized total immune cell subset count for the data provided in each study.

From these standardized total immune cell subset counts, we are able to determine the proportion of immune cell subsets within the brain by simply dividing the standardized count by 1 x 10^5 total cells collected to obtain percentages (**Figure 6**, **Suppl. Table 3**). As expected, the top three immune cell subsets found within WT/control mouse brain were TMEM119$^+$ IBA1$^-$ “steady state/ramified” microglia (28.5% ± 33.0), S100B$^+$ only astrocytes (12.7% ± 0), and GFAP$^+$ only astrocytes (8.30% ± 0). Out of the non-neural specific immune cells, bulk CD4$^+$ T cells (6.41% ± 6.15) and bulk CD8$^+$ T

cells (4.00% ± 5.34) were most often counted within mouse brain compared to other adaptive/innate immune cells. Overall, we were able to calculate the average percentage of immune cells found within WT/control mouse brain from the 52 selected studies. Hence, we are able to report a more reliable estimate of the immune cell composition within mouse brain despite still high SD values.

3.6 Evaluating risk of bias of all included studies

As per PRISMA and Cochrane criteria for systematic reviews, it is important to evaluate the risk of bias for all studies cited (20,21,24,83). Here we utilize the SYRCLE's risk of bias tools for animal studies (24) to create a summary graph and "stop-light" figure (**Figure 7**) to highlight the overall bias of each study assessed within the following domains: D1: Sequence Generation (randomization methods used to choose animals for comparable groups); D2: Baseline Characteristics (full description of animal characteristics from all comparable groups); D3: Allocation Concealment (methods used to conceal how animals are distributed to researchers, i.e. using a coding method for each animal) ; D4: Random Housing (housing all animal groups randomly within the animal room); D5: Blinding (blinding methods used on researchers, such as blinding the knowledge of intervention or transgenic model used and blinding the outcome assessors); D6: Random Outcome Assessment (methods on how the animals were selected at random for outcome assessment); D7: Incomplete Outcome Data (description of the completeness of the data outcome, i.e., stating if data was excluded or if animals were removed from study at any point); D8: Selective Outcome Reporting (the completeness of the study protocols); D9: Other Sources of Bias (examples include: confounders, contamination problems, analysis errors, design-specific risk of bias, etc.).

The overall bias of all selected studies was deemed predominantly "unclear" (~over 50%) due to lack of reporting on specific data/methodology required to pass the "high" or "low" bias questionnaire in each study (**Figure 7**). The most bias domains (~over 50%) from the selected studies was Baseline

Characteristics (i.e. it was largely unclear how sex, age, weight or other baseline characteristics or confounders were adjusted for in each analysis) and Incomplete Outcome Data (i.e. it was generally unclear whether all animals were included in each analysis, and if not, whether there any report on why they were missing outcome data or how that missing data influenced the study). The lowest bias domain (~over 75%) was Selective Outcome Reporting (i.e. did the results reported reflect on the methods described in the selective studies). Overall, the reported bias from all included studies were largely considered to be "unclear" due to the lack of reporting and transparency in the methods and results described.

4 Discussion and Recommendations

A prominent role for the innate and acquired immune system in brain health, neurologic and age-associated neurodegenerative disorders has become increasing apparent. In part, this has been driven by the immunologic role of several variant gene discoveries including triggering receptor expressed on myeloid cells 2 (*TREM2*) in Alzheimer's disease, granulin (*GRN*) in frontotemporal dementia and leucine rich repeat kinase 2 (*LRRK2*) in Parkinson's disease (84–87). Despite this burgeoning interest in neuroimmunology, and many published studies, results from flow cytometry immunophenotyping from homogenized mouse brain are highly variable. Although this does not invalidate 'within study' comparisons of specific immune subsets, such variability is a challenge for reproducibility, meta-analysis across studies and interpretation (27–78). Reliable data on residential and infiltrating immune cells within WT/control mouse brain would be of benefit (1–10). One step towards that goal is standardized reporting of flow cytometry methods and results as well as requiring to become a prerequisite for peer-reviewed publications. In this systematic review, we demonstrate most studies that apply flow cytometry methods to neurology and neuroimmunology, specifically to homogenized

mouse brain, share little to no consensus on methods, analysis or results. Here we summarize our findings and make a series of recommendations for future studies (**Table 1**).

We retrieved 52 neurological/neuroimmunology studies that utilized flow cytometry to identify or sort multiple immune cell subsets from WT/control mouse brain, which generally compared within study results to an experimental mouse model (27–78). We compared mouse strains and perfusion and tissue processing methods, and note the age of mice and methods for tissue homogenization are variable. However, younger mice have a different immune landscape to older animals (88–91). Vivarium conditions, such as group housing within ventilated racks in a pathogen free barrier facility versus more conventional non-barrier non-ventilated caging, are seldom documented. Housing conditions, age and gender influences the immune cell subsets that can be identified by flow cytometry, and should be carefully considered, documented in experimental protocols and, whenever possible, adjusted for as a covariate in subsequent analyses. When deciding on immune cell isolation methods for mouse brains both mechanical homogenization or/and enzymatic tissue digestion are appropriate. Nevertheless, each approach has pros and cons on immune cell retrieval and phenotypic expression, and depending on the specific research question, must be carefully considered (92–94).

Once the mouse lines and homogenization/isolation methods were analyzed, we compared flow cytometry techniques and data reporting across the 52 studies. Cytometers/FACS sorters come in a variety of makes and models, but essentially do the same function, and should be calibrated using universal standards (82,95,96). Many useful guidelines exist for reporting and include the Minimum Information about a Flow Cytometry Experiment (MIFlowCyt) criteria (26,82,95,97). These recommend researchers present flow cytometry data and methods by reporting: 1) sample/specimen used for experiments; 2) how the samples were treated (storage, processing, stained, etc.); 3) what reagents were used and which antibody clones; 4) what controls were used (unstained controls,

FMOs, single color controls, etc.) with a demonstration of the full gating strategy for each panel; 5) what instrument was used and details about it; 6) how many total cells and/or live cells were collected in each sample; 7) what analysis software was used and how compensation was calculated. Greater adherence would enable more reliable and accurate results, increase reproducibility and subsequent meta-analysis.

In the 52 selected studies, we next examined the median and average count and percentages of immune cell subsets reported from a WT/control mouse brain. The immune cell subsets selected (**Figure 5**, **Figure 6**, **Suppl. Table 3**) consist of brain/CNS-only residential immune cells (astrocytes and microglia) and immune cells considered to be both residential and peripheral (i.e. T cells, B cells, macrophages, NK cells) (1–10). As expected, of all the immune subsets examined, astrocytes and microglia are the most populated immune cells within WT/control mouse brain (15,27,28,76–78). It is of note that three different astrocyte phenotypes were documented ($S100B^+$ only, $GFAP^+$ only, and $GFAP^+$ $S100B^+$ cells). However, some astrocytes do not readily express GFAP and S100B is expressed more in mature astrocytes (98–101). Similar observations were made for microglia subsets; TMEM119 is found expressed in more stable, non-reactive microglia, whereas IBA1 can be expressed in more active microglia and other phagocytic cells (102–105). For other immune cell subsets, T cells make up the second most abundant immune cell within WT/control mouse brains, with more bulk $CD4^+$ T cells (29–39). In the brain, it is likely both $CD4^+/CD8^+$ T cells are comprised of resident memory T cells (T_{RM}) and might be classified as an even more specialized subset (i.e. T_{CM}, T_{EM}, and T_{EMRA}) (106–108). For the innate immune cell populations (excluding microglia and astrocytes), NK cells were observed more frequently in WT/control mouse brain than other innate immune cells (35,48–53). Many studies report NK cells as most abundant within the brain's parenchyma, and more often than other innate immune populations (excluding microglia and astrocytes) or adaptive immune cells (T cell and B cells) (109–111). NK cells were the most reported

innate immune cell subset within WT/control mouse brains in the 52 studies reviewed, but there were still more bulk $CD4^+/CD8^+$ T cell counts reported. The presence of less abundant immune cell subsets found within the brain, or infiltrating the brain, including specific $CD4^+$ T cell subsets, T cell memory subsets, and DCs, were also assessed. Unpredictably, it appears that T_{H1} T cells are more abundant in WT/control mouse brains than T_{H2} T cells (not reported in the 52 selected studies) (29,42). Conventionally, the T_{H1}/T_{H2} ratio is used to determine whether an individual has a bacterial/viral infection (higher ratios are indicative or greater infection) although higher ratios of these subsets are also found in aged subjects, once again highlighting the importance of defining age in studies of immunity (112). None of the 52 studies included reported specific T cell memory subsets besides bulk T_{EM} $CD4^+/CD8^+$ T cells (32) within WT/control mice. Given the importance of specific T cell memory subsets to overall immunity, future flow cytometry analysis of the brain may benefit from their inclusion. Surprisingly, a few reports listed migratory/residential DCs within WT/control mouse brains, albeit at extremely low levels (35,54–57), as microglia are thought to mediate brain immune surveillance (113–115).

Our systematic review has some limitations. Our analysis and database search were not automated to update figures from more recent research (116,117) and potentially, this may be considered a selection bias. The key word searches we conducted for each immune cell subset has been reported in our methodology, however, different variations of these words or use of other abbreviations when searching could alter what literature is identified in each database, thus could also be considered some level of bias. Several of the studies included also failed to report sufficient details within their main text, figures, or supplementary materials, and whenever possible that data was extrapolated. Nevertheless, there was tremendous variability in immune cell subset counts in the 52 studies reviewed, where SD often exceeded mean measures, thus the overall calculated medians with IQRs were reported more thoroughly in this review. Although heterogeneity in instrumentation is

unavoidable and necessary in experimental design, and within study comparisons are still valid, it would be helpful to uniformly define how immunophenotyping is reported, including vivarium housing, age, sex, and strain. There needs to be greater effort to standardized total immune cell counts and to standardize the reporting of specific immune cell subset counts. From our analysis, we have sought to make a series of criteria and recommendations to aid interpretation of results, reproducibility and meta-analysis (**Table 1**). Adherence to reporting guidelines will ultimately improve our understanding of the dynamic role of immunity in mouse brain.

5 Figure Legends

Figure 1. Prisma Flow Diagram. Guidelines provided by PRISMA (21).

Figure 2. Mouse information reported between studies. Reported baseline mouse information described as percentages out of the 52 studies: **A.** mouse strains; **B.** mouse ages; and **C.** mouse genders.

Figure 3. Brain tissue dissociation and cell isolation methods reported between studies. Tissue processing techniques were reported as percentages from the 52 studies: **A.** brain dissociation filters utilized; **B.** digestion enzymes used for brain homogenization; and **C.** Percoll gradients used to remove myelin layer.

Figure 4. Reporting of flow cytometry results and cell counts between the studies. Differences in flow cytometry results and cell counts reported as within study percentages (n=52 studies): **A.** gating strategy used; **B.** total cells per sample collected from flow cytometer/sorter; and **C.** total immune cell subset counts derived from the live cell gate.

Figure 5. Calculated medians with interquartile ranges (IQRs) of immune cells quantified by flow cytometry within wild-type/control mouse brains. Medians with IQRs (defined as: 75th percentile upper quartile [Q3] – 25th percentile lower quartile [Q1]) of immune cell subset counts found with wild-type (WT)/control homogenized mouse brain were calculated from data extrapolated from the 52 studies selected for inclusion in this systematic review. Immune cell subsets were organized as: **A.** bulk adaptive immune cells; **B.** specialized T cells; **C.** innate immune cells; and **D.** brain-specific immune cells. Total n-values (number of studies for each identified subset) are reported along with the median and IQR for each immune subset above each bar graph.

Figure 6. Standardized total cell percentages of immune cells quantified by flow cytometry within wild-type/control mouse brains. Estimated percentages of immune cell subset counts found within wild-type (WT)/control homogenized mouse brain were calculated from data extrapolated from the 52 studies selected for inclusion in this systematic review. The equations used to determine the standardized cell counts can be found in the Methods section. Briefly, "raw" total immune cell subset count and "raw" total cell count collected via flow cytometry were standardized assuming 1 x 10^5 total cells were collected. Results were reported as combined means of percentages with standard deviations (±SD) from the standardized totals from each study assuming 1 x 10^5 total cells were collected.

Figure 7. SYRCLE's risk of bias: Tools for animal studies summarized for each study. Both the summary graph and "stop-light" figure were created via the *robvis* R package and Shiny web app (25). Criteria are based upon the Systematic Review Centre for Laboratory animal Experimentation (SYRCLE) (23) methodology to detect bias (24). All 52 studies selected were reviewed and analyzed using SYRCLE criteria domains: D1: Sequence Generation; D2: Baseline Characteristics; D3: Allocation Concealment; D4: Random Housing; D5: Blinding; D6: Random Outcome Assessment; D7: Incomplete Outcome Data; D8: Selective Outcome Reporting; and D9: Other Sources of Bias. Red: High Bias; Yellow: "Unclear" Bias; Green: Low Bias.

Tables

Table 1. Minimum recommendations and sources for standards for future mouse brain flow cytometry reports

Table 2. Minimum recommendations and sources for standards for future mouse brain flow cytometry reports(4,5,13,15,26,82,88–91,95)	
Criteria	**Recommendations and Notes**
Mouse Strain	• Report background mouse strain being used, as different mouse strains have different immune backgrounds. • Ensure a WT or a non-treated mouse strain is used within the study and are housed in the same vivarium as transgenic/treated mice in order to create more accurate comparisons. • Report any specific detail of the vivarium and what caging conditions the mice were in. • DO NOT switch mouse strains up in the middle of experimentation within the study, as immune profiles will vary drastically. • As much genetic, phenotypic, and supplier information should be provided from each mouse strain used.
Mouse Age	• Report the ages of the mice used for the study, as immune profiles are altered by age. • For a more naïve, younger immune cell population, it is best to utilize mice aged ~3 months. • For a more mature, older immune cell population, it is best to utilize mice aged ~15 months. • Age can affect neurological phenotype and behavior; thus, need to be included as a confounder.
Mouse Gender	• Report the gender of the mice used, as male and female mice have different immune responses. • Ensure that the same gender of mice is used throughout all experiments within the study, unless the study is focused on gender differences. • Use equal N-values of male and female for each experiment conducted.
Perfusion Techniques	• Perfusion is recommended before conducting brain homogenization, as to avoid having circulating blood/immune cell contamination within the brains. • Use cold Hank's balanced salt solution (HBSS) with 10% serum (i.e. heat-inactive fetal bovine serum [FBS], mouse serum, etc.) for heart puncture perfusion of the mice, as this solution is best for keeping both residential immune cells and neurological cells intact and remain viable for flow cytometry. Saline with 10% serum could be used as well. • Using 4% paraformaldehyde (PFA) in any perfusion mixture will affect flow cytometry staining and should be done AFTER staining for surface antigens.
Brain Dissociation and Cell Isolation Techniques	• Choosing to do mechanical homogenization (i.e. Dounce tissue grinder, bead beating, sonication, etc.), enzymatic homogenization (i.e. collagenase, DNase I, trypsin-EDTA, etc.), or the combination of both can alter the phenotypes of immune cells, thus the it is important to describe which technique was used. • Use one or more cell strainers (preferably using a 100 µm filter first, then a 70 µm filter) in order to remove as much excess dead cells, fats, myelin, etc. as possible, as these components will alter flow cytometry collection and readings.

	• Use an isotonic Percoll gradient in order to isolate immune cells and other cells of interest, where at a minimum a 37% isotonic Percoll gradient should be used in order to remove all of the myelin (top layer) and isolate all brain cells (bottom layer/cell pellet). • A 30%/37%/70% isotonic Percoll solution is also recommended if microglia isolation is the only objective.
Flow Cytometer/Sorter Equipment and Analysis Software Reporting	• Report the exact specifications of the flow cytometer/sorter used in the study. • DO NOT switch between cytometers/sorters throughout experimentation, as different models can produce different results. It is also recommended that calibration and optimization of the machine is done every day if possible in order to get accurate and concise results. • Report flow cytometry antibody information, such as clone ID, fluorophore conjugated, targets, company it is bought from, etc. • Analysis software and version number should be reported due to each software having slightly different analysis methods.
Flow Cytometry Result Reporting	• Include a representation of the entire gating strategy (from forward scatter/side scatter, to single cells, to live dead, to beginning of gating strategy and beyond) for each type of experiment conduct. For these figures, it is recommended they come from a WT/non-treated control mouse. • State that the results provided are standardized and comparable to multiple flow cytometry controls, such as unstained, FMO, and single-color controls. It is also highly recommended that, at a minimum, that either unstained and/or FMO control gating should be included within the report. • For each represented gating strategy, provide, if possible, both cell counts and cell percentages for each gate reported. • For histogram presentations, show representations by way of stacked histograms, which includes an unstained and FMO histogram along with the subjects' histograms. It is also recommended to indicate MFI readings for each histogram to be included. • Reporting total cells per sample collected by flow cytometry should be included. This can be reported as a unified cell count (i.e. all samples had 1×10^5 cells collected during flow cytometry) or each individual sample has the number of cells collected included in the results. • Use a live/dead dye in order to separate out only living cells in order for an accurate gating strategy and cell count. It is also suggested to include the total amount of live cells counted on average or from each sample in the methods or result section. • Report cell subsets as either total cell counts or by percentages derived from either live cells or from total cells collected. It is NOT recommended to report only subset percentages from a single gate after live/dead gating, i.e. reporting cell percentages only deriving from $CD45^+$ gating, in the main text or in figures. • Methods used to describe how cell counts were reported (i.e. by use of flow cytometry cell counting beads, counts provided by the machine, counts calculated, etc.) or how MFI's were calculated is recommended.

Conflict of Interest

The authors declare that the research was conducted in the absence of any commercial or financial relationships that could be construed as a potential conflict of interest.

Author Contributions

RCS and MJF performed the search and analysis of this systematic review. RCS and MJF contributed equally on the conception, design, organization. All authors contributed to manuscript revision, read, and approved the submitted version.

Funding

MJF is supported by the Lee and Lauren Fixel Chair for Parkinson's disease research.

Acknowledgments

The authors would like to thank John P.A. Ioannidis from the Meta-Research Innovation Center at Stanford (METRICS) and the Departments of Medicine, Epidemiology and Population Health, Biomedical Data Science, and Statistics at Stanford University, Stanford, CA., for their insights on systematic reviews and meta-analysis. The authors would also like to thank the entire Farrer lab at the University of Florida for their encouragement and support to perform this systematic review.

Data Availability Statement

All relevant data is contained within the article: The original contributions presented in the study are included in the article/supplementary material, further inquiries can be directed to the corresponding author/s.

Figures

Figure 1

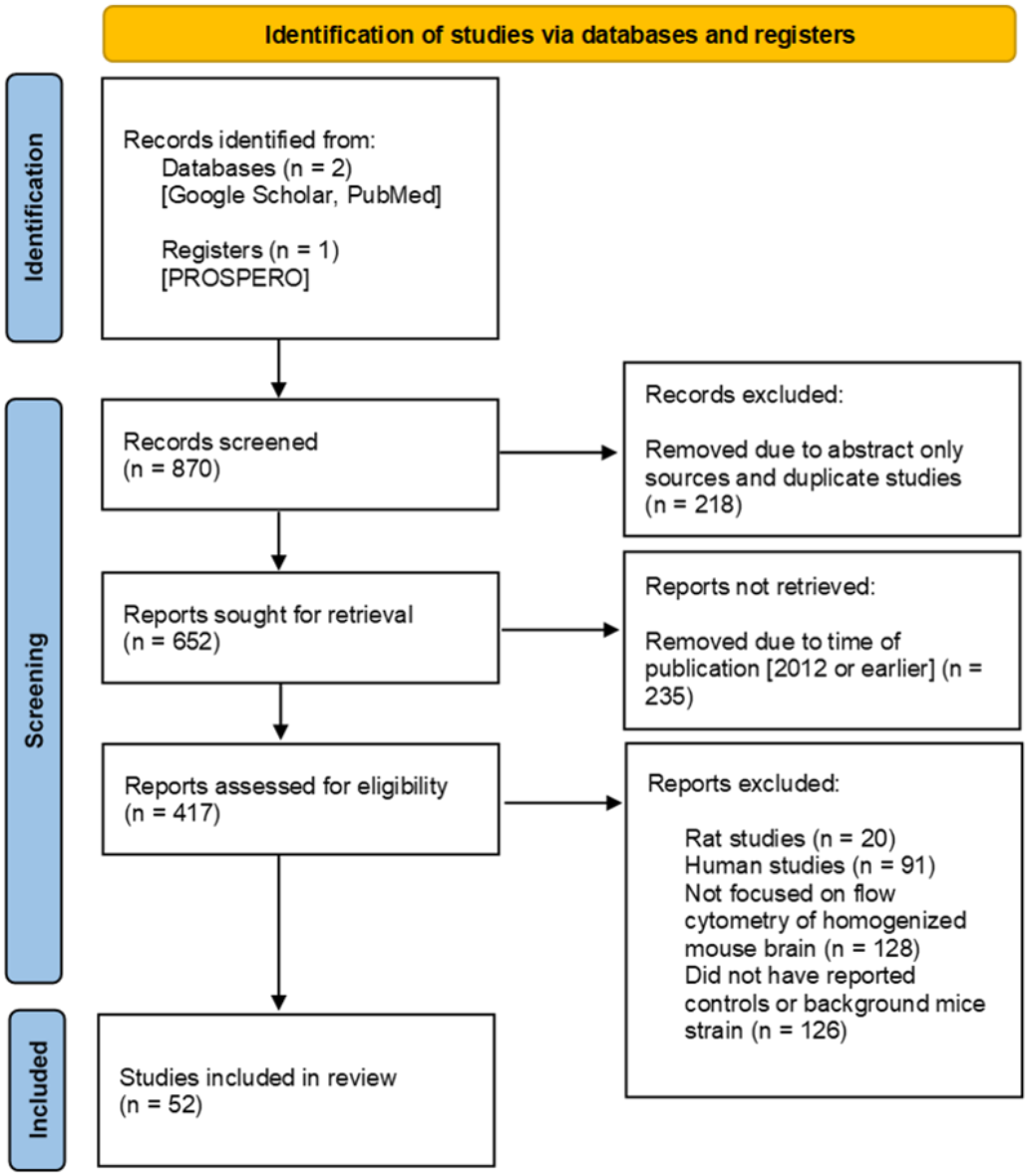

Figure 2

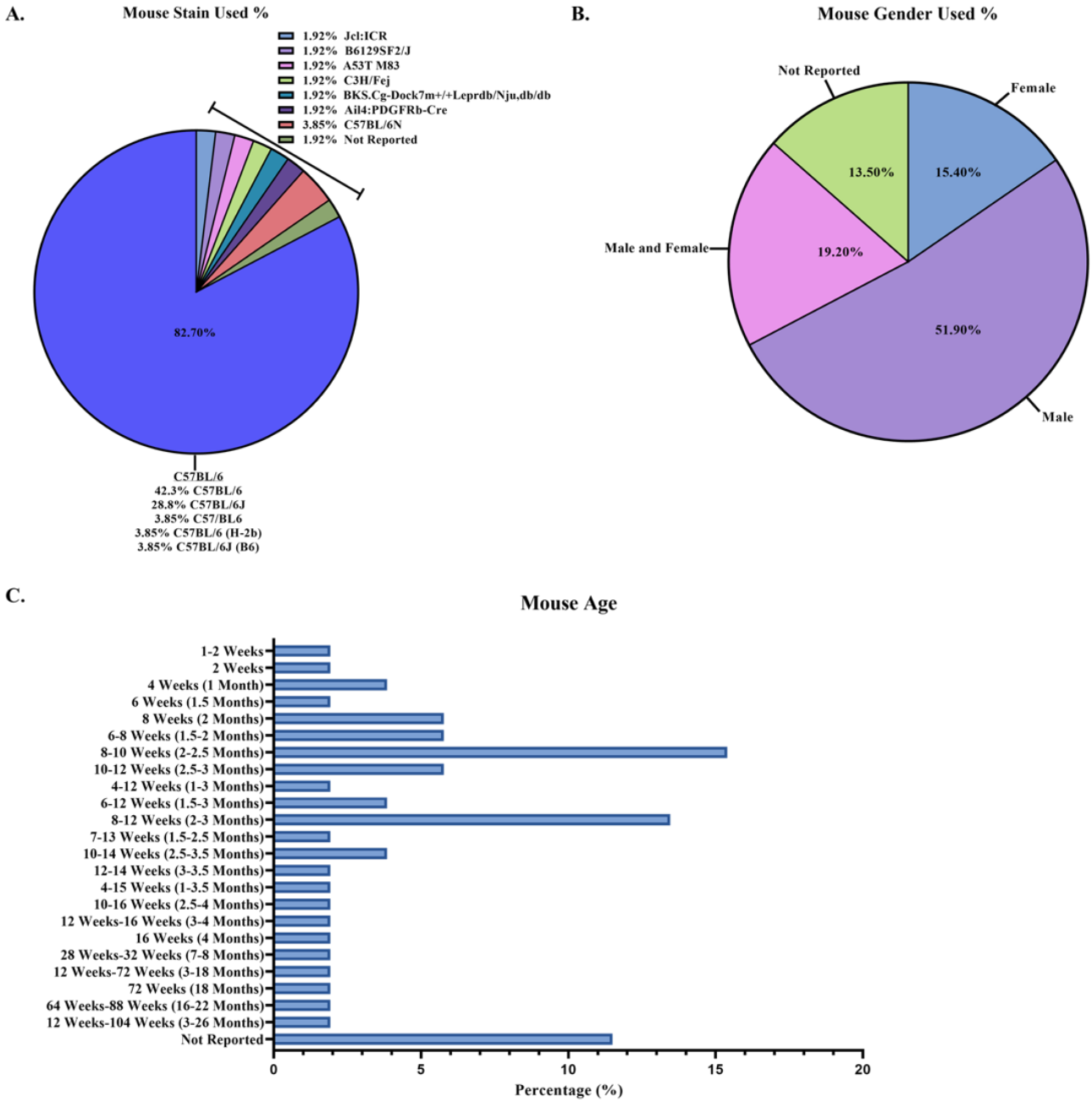
A.
Mouse Stain Used %
1.92% Jcl:ICR
1.92% B6129SF2/J
1.92% A53T M83
1.92% C3H/Fej
1.92% BKS.Cg-Dock7m+/+Leprdb/Nju,db/db
1.92% Ail4:PDGFRb-Cre
3.85% C57BL/6N
1.92% Not Reported
82.70%
C57BL/6
42.3% C57BL/6
28.8% C57BL/6J
3.85% C57/BL6
3.85% C57BL/6 (H-2b)
3.85% C57BL/6J (B6)
B.
Mouse Gender Used %
Not Reported
Female
13.50%
15.40%
Male and Female
19.20%
51.90%
Male
C.
Mouse Age
1-2 Weeks
2 Weeks
4 Weeks (1 Month)
6 Weeks (1.5 Months)
8 Weeks (2 Months)
6-8 Weeks (1.5-2 Months)
8-10 Weeks (2-2.5 Months)
10-12 Weeks (2.5-3 Months)
4-12 Weeks (1-3 Months)
6-12 Weeks (1.5-3 Months)
8-12 Weeks (2-3 Months)
7-13 Weeks (1.5-2.5 Months)
10-14 Weeks (2.5-3.5 Months)
12-14 Weeks (3-3.5 Months)
4-15 Weeks (1-3.5 Months)
10-16 Weeks (2.5-4 Months)
12 Weeks-16 Weeks (3-4 Months)
16 Weeks (4 Months)
28 Weeks-32 Weeks (7-8 Months)
12 Weeks-72 Weeks (3-18 Months)
72 Weeks (18 Months)
64 Weeks-88 Weeks (16-22 Months)
12 Weeks-104 Weeks (3-26 Months)
Not Reported
0
5
10
15
20
Percentage (%)

Figure 3

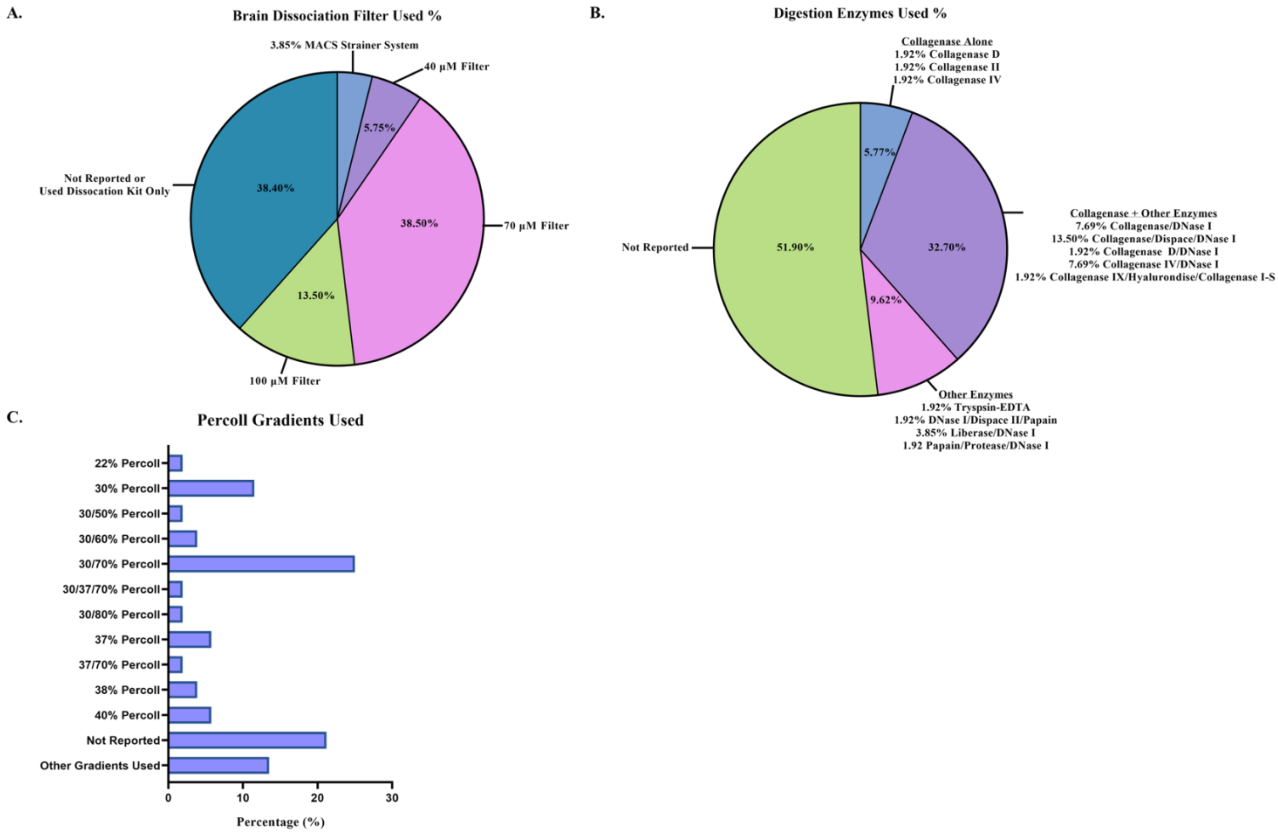
A.
Brain Dissociation Filter Used %
3.85% MACS Strainer System
40 µM Filter
5.75%
Not Reported or
Used Dissocation Kit Only
38.40%
38.50%
70 µM Filter
13.50%
100 µM Filter
B.
Digestion Enzymes Used %
Collagenase Alone
1.92% Collagenase D
1.92% Collagenase II
1.92% Collagenase IV
5.77%
Collagenase + Other Enzymes
7.69% Collagenase/DNase I
13.50% Collagenase/Dispace/DNase I
1.92% Collagenase D/DNase I
7.69% Collagenase IV/DNase I
1.92% Collagenase IX/Hyalurondise/Collagenase I-S
Not Reported
51.90%
32.70%
9.62%
Other Enzymes
1.92% Tryspsin-EDTA
1.92% DNase I/Dispace II/Papain
3.85% Liberase/DNase I
1.92 Papain/Protease/DNase I
C.
Percoll Gradients Used
22% Percoll
30% Percoll
30/50% Percoll
30/60% Percoll
30/70% Percoll
30/37/70% Percoll
30/80% Percoll
37% Percoll
37/70% Percoll
38% Percoll
40% Percoll
Not Reported
Other Gradients Used
0
10
20
30
Percentage (%)

Figure 4

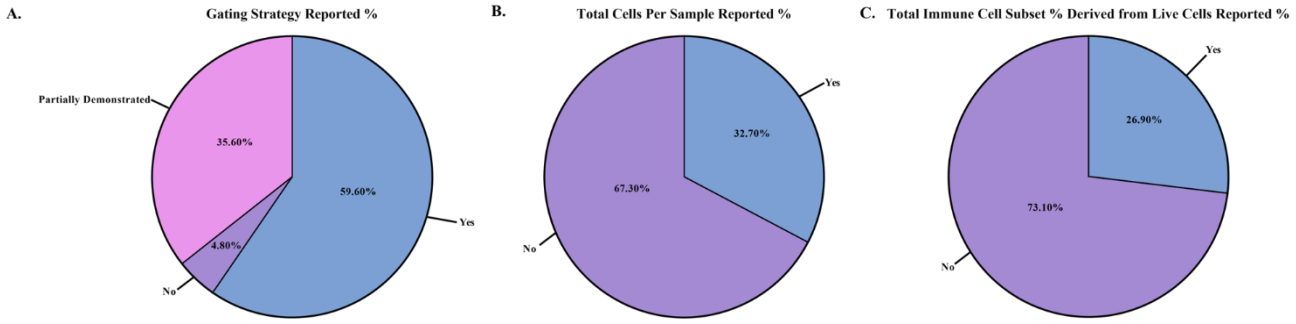
A.
Gating Strategy Reported %
Partially Demonstrated
35.60%
59.60%
Yes
4.80%
No
B.
Total Cells Per Sample Reported %
Yes
32.70%
67.30%
No
C.
Total Immune Cell Subset % Derived from Live Cells Reported %
Yes
26.90%
73.10%
No

Figure 5

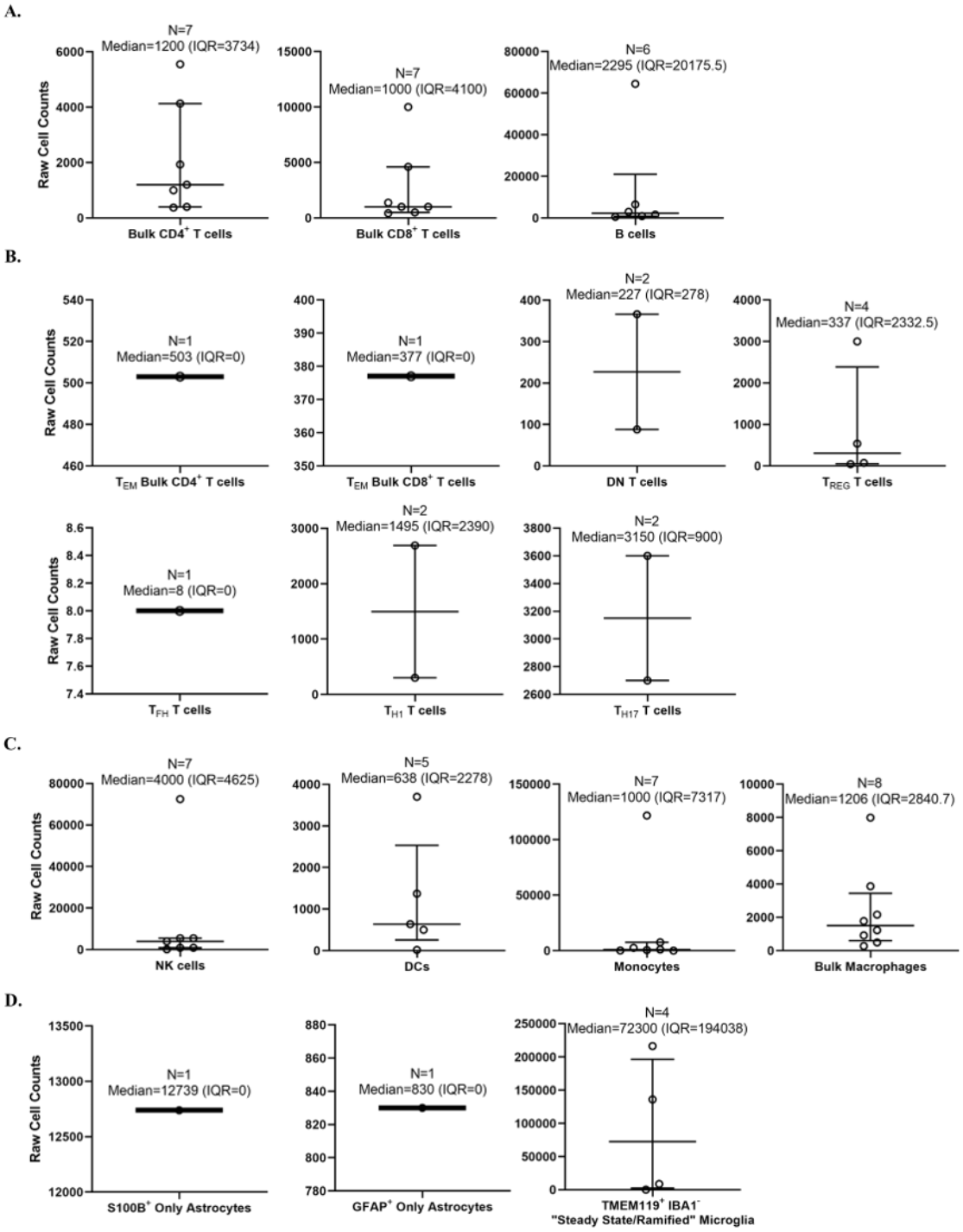
A.
Raw Cell Counts
N=7
Median=1200 (IQR=3734)
Bulk CD4+ T cells
N=7
Median=1000 (IQR=4100)
Bulk CD8+ T cells
N=6
Median=2295 (IQR=20175.5)
B cells
B.
N=1
Median=503 (IQR=0)
TEM Bulk CD4+ T cells
N=1
Median=377 (IQR=0)
TEM Bulk CD8+ T cells
N=2
Median=227 (IQR=278)
DN T cells
N=4
Median=337 (IQR=2332.5)
TREG T cells
N=1
Median=8 (IQR=0)
TFH T cells
N=2
Median=1495 (IQR=2390)
TH1 T cells
N=2
Median=3150 (IQR=900)
TH17 T cells
C.
N=7
Median=4000 (IQR=4625)
NK cells
N=5
Median=638 (IQR=2278)
DCs
N=7
Median=1000 (IQR=7317)
Monocytes
N=8
Median=1206 (IQR=2840.7)
Bulk Macrophages
D.
N=1
Median=12739 (IQR=0)
S100B+ Only Astrocytes
N=1
Median=830 (IQR=0)
GFAP+ Only Astrocytes
N=4
Median=72300 (IQR=194038)
TMEM119+ IBA1-
"Steady State/Ramified" Microglia

Figure 6

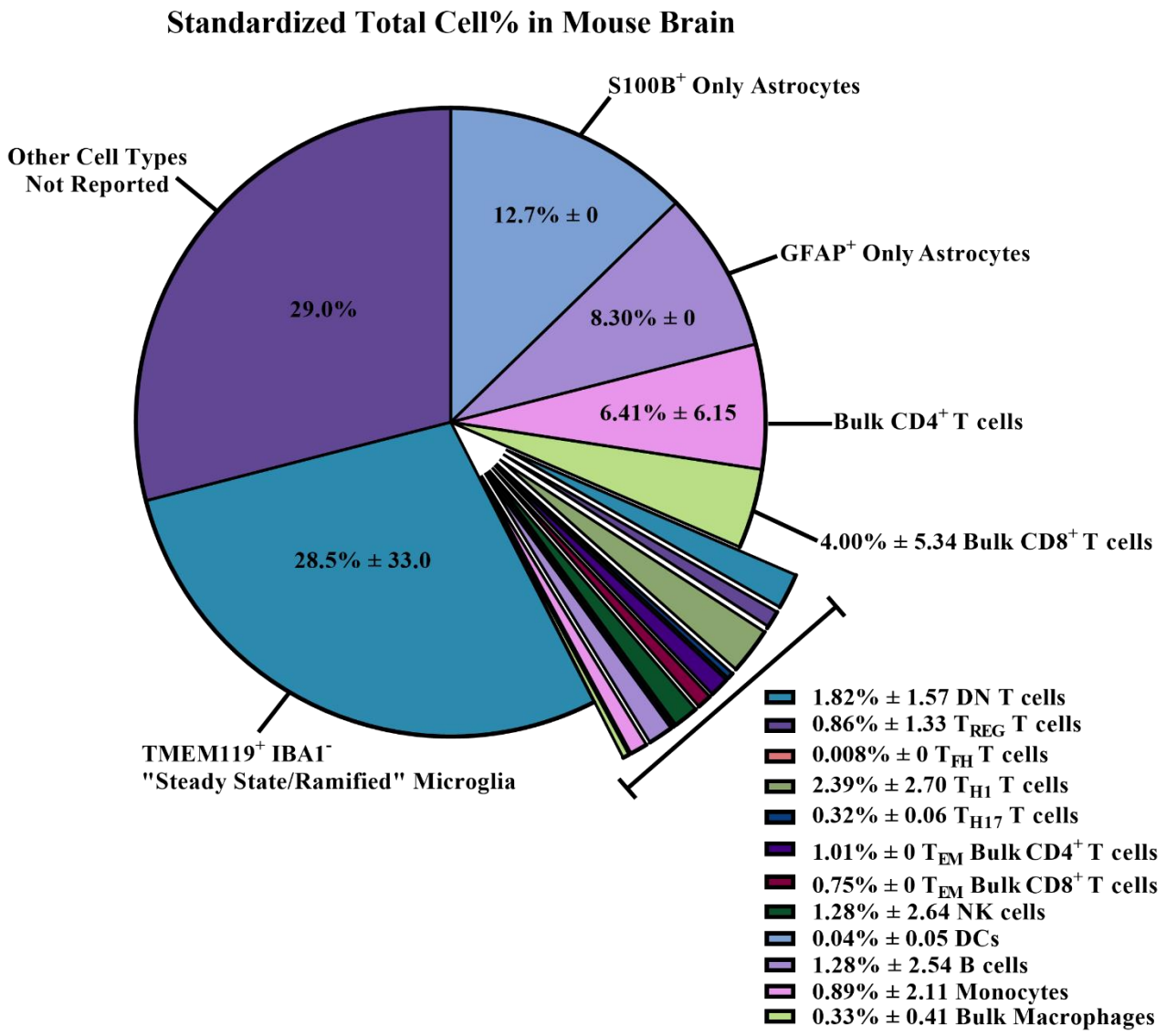
Standardized Total Cell% in Mouse Brain
S100B+ Only Astrocytes
12.7% ± 0
GFAP+ Only Astrocytes
8.30% ± 0
Bulk CD4+ T cells
6.41% ± 6.15
4.00% ± 5.34 Bulk CD8+ T cells
Other Cell Types Not Reported
29.0%
TMEM119+ IBA1- "Steady State/Ramified" Microglia
28.5% ± 33.0
1.82% ± 1.57 DN T cells
0.86% ± 1.33 TREG T cells
0.008% ± 0 TFH T cells
2.39% ± 2.70 TH1 T cells
0.32% ± 0.06 TH17 T cells
1.01% ± 0 TEM Bulk CD4+ T cells
0.75% ± 0 TEM Bulk CD8+ T cells
1.28% ± 2.64 NK cells
0.04% ± 0.05 DCs
1.28% ± 2.54 B cells
0.89% ± 2.11 Monocytes
0.33% ± 0.41 Bulk Macrophages

Figure 7

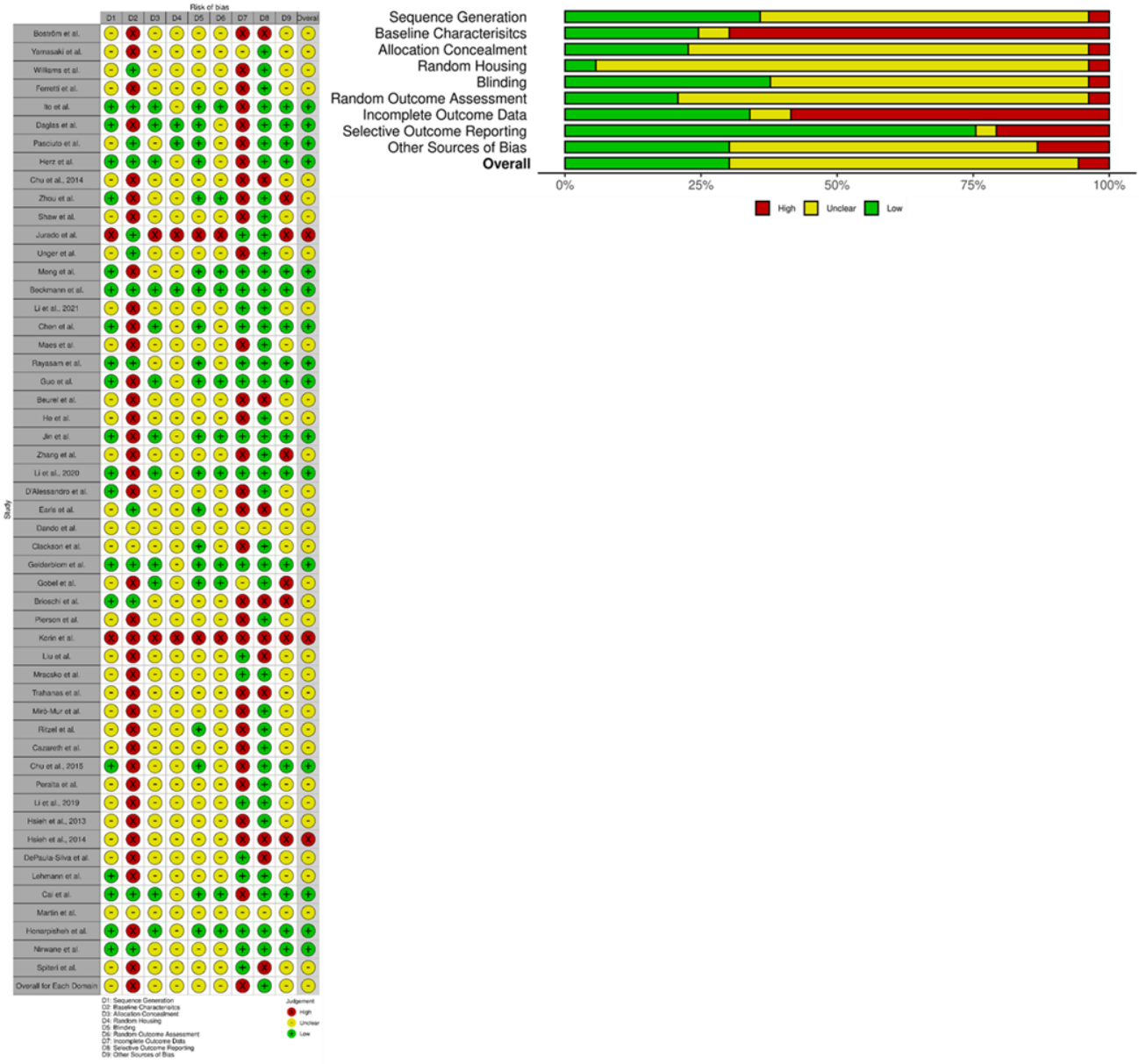
Risk of bias
D1 D2 D3 D4 D5 D6 D7 D8 D9 Overal
Study
Sequence Generation
Baseline Characterisitcs
Allocation Concealment
Random Housing
Blinding
Random Outcome Assessment
Incomplete Outcome Data
Selective Outcome Reporting
Other Sources of Bias
Overall
0%
25%
50%
75%
100%
High
Unclear
Low
D1: Sequence Generation
D2: Baseline Characteristics
D3: Allocation Concealment
D4: Random Housing
D5: Blinding
D6: Random Outcome Assessment
D7: Incomplete Outcome Data
D8: Selective Outcome Reporting
D9: Other Sources of Bias
Judgement
High
Unclear
Low

References

1. Dawson TM, Golde TE, Lagier-Tourenne C. Animal models of neurodegenerative diseases. *Nat Neurosci* (2018) 21:1370–1379. doi: 10.1038/s41593-018-0236-8

2. Chesselet M-F, Carmichael ST. Animal Models of Neurological Disorders. *Neurotherapeutics* (2012) 9:241–244. doi: 10.1007/s13311-012-0118-9

3. Hafezparast M, Ahmad-Annuar A, Wood NW, Tabrizi SJ, Fisher EM. Mouse models for neurological disease. *Lancet Neurol* (2002) 1:215–224. doi: 10.1016/S1474-4422(02)00100-X

4. Croxford JL, Miyake S. "Animal Models for the Study of Neuroimmunological Disease.," *Neuroimmunological Diseases*. Tokyo: Springer Japan (2016). p. 33–54 doi: 10.1007/978-4-431-55594-0_3

5. da Silva APB, Silva RBM, Goi LDS, Molina RD, Machado DC, Sato DK. Experimental Models of Neuroimmunological Disorders: A Review. *Front Neurol* (2020) 11: doi: 10.3389/fneur.2020.00389

6. Grotemeyer A, McFleder RL, Wu J, Wischhusen J, Ip CW. Neuroinflammation in Parkinson's Disease – Putative Pathomechanisms and Targets for Disease-Modification. *Front Immunol* (2022) 13: doi: 10.3389/fimmu.2022.878771

7. Saito T, Saido TC. Neuroinflammation in mouse models of Alzheimer's disease. *Clin Exp Neuroimmunol* (2018) 9:211–218. doi: 10.1111/cen3.12475

8. Passaro AP, Lebos AL, Yao Y, Stice SL. Immune Response in Neurological Pathology: Emerging Role of Central and Peripheral Immune Crosstalk. *Front Immunol* (2021) 12: doi: 10.3389/fimmu.2021.676621

9. Tan EK, Chao YX, West A, Chan LL, Poewe W, Jankovic J. Parkinson disease and the immune system — associations, mechanisms and therapeutics. *Nat Rev Neurol* (2020) 16:303–318. doi: 10.1038/s41582-020-0344-4

10. Ma Q, Xing C, Long W, Wang HY, Liu Q, Wang R-F. Impact of microbiota on central nervous system and neurological diseases: the gut-brain axis. *J Neuroinflammation* (2019) 16:53. doi: 10.1186/s12974-019-1434-3

11. Hu P, Zhang W, Xin H, Deng G. Single Cell Isolation and Analysis. *Front Cell Dev Biol* (2016) 4: doi: 10.3389/fcell.2016.00116

12. Lanz T V., Pröbstel A-K, Mildenberger I, Platten M, Schirmer L. Single-Cell High-Throughput Technologies in Cerebrospinal Fluid Research and Diagnostics. *Front Immunol* (2019) 10: doi: 10.3389/fimmu.2019.01302

13. Drescher H, Weiskirchen S, Weiskirchen R. Flow Cytometry: A Blessing and a Curse. *Biomedicines* (2021) 9:1613. doi: 10.3390/biomedicines9111613

14. de Graaf MT, de Jongste AHC, Kraan J, Boonstra JG, Smitt PAES, Gratama JW. Flow cytometric characterization of cerebrospinal fluid cells. *Cytometry B Clin Cytom* (2011) 80B:271–281. doi: 10.1002/cyto.b.20603

15. Martin D, Xu J, Porretta C, Nichols CD. Neurocytometry: Flow Cytometric Sorting of Specific Neuronal Populations from Human and Rodent Brain. *ACS Chem Neurosci* (2017) 8:356–367. doi: 10.1021/acschemneuro.6b00374

16. Brioschi S, d'Errico P, Amann LS, Janova H, Wojcik SM, Meyer-Luehmann M, Rajendran L, Wieghofer P, Paolicelli RC, Biber K. Detection of Synaptic Proteins in Microglia by Flow Cytometry. *Front Mol Neurosci* (2020) 13: doi: 10.3389/fnmol.2020.00149

17. Mrdjen D, Pavlovic A, Hartmann FJ, Schreiner B, Utz SG, Leung BP, Lelios I, Heppner FL, Kipnis J, Merkler D, et al. High-Dimensional Single-Cell Mapping of Central Nervous System Immune Cells Reveals Distinct Myeloid Subsets in Health, Aging, and Disease. *Immunity* (2018) 48:380-395.e6. doi: 10.1016/j.immuni.2018.01.011

18. Kim H, Sefcik JS, Bradway C. Characteristics of Qualitative Descriptive Studies: A Systematic Review. *Res Nurs Health* (2017) 40:23–42. doi: 10.1002/nur.21768

19. Hooijmans CR, IntHout J, Ritskes-Hoitinga M, Rovers MM. Meta-Analyses of Animal Studies: An Introduction of a Valuable Instrument to Further Improve Healthcare. *ILAR J* (2014) 55:418–426. doi: 10.1093/ilar/ilu042

20. Vesterinen HM, Sena ES, Egan KJ, Hirst TC, Churolov L, Currie GL, Antonic A, Howells DW, Macleod MR. Meta-analysis of data from animal studies: A practical guide. *J Neurosci Methods* (2014) 221:92–102. doi: 10.1016/j.jneumeth.2013.09.010

21. Moher D, Liberati A, Tetzlaff J, Altman DG. Preferred Reporting Items for Systematic Reviews and Meta-Analyses: The PRISMA Statement. *PLoS Med* (2009) 6:e1000097. doi: 10.1371/journal.pmed.1000097

22. Clarke M, Oxman A, Paulsen E, Higgins J, Green S. Guide to the contents of a Cochrane Methodology protocol and review. *The Cochrane Collaboration* (2020) 5.1.0:

23. Munn Z, Stern C, Aromataris E, Lockwood C, Jordan Z. What kind of systematic review should I conduct? A proposed typology and guidance for systematic reviewers in the medical and health sciences. *BMC Med Res Methodol* (2018) 18:5. doi: 10.1186/s12874-017-0468-4

24. Hooijmans CR, Rovers MM, de Vries RB, Leenaars M, Ritskes-Hoitinga M, Langendam MW. SYRCLE's risk of bias tool for animal studies. *BMC Med Res Methodol* (2014) 14:43. doi: 10.1186/1471-2288-14-43

25. McGuinness LA, Higgins JPT. Risk-of-bias VISualization (robvis): An R package and Shiny web app for visualizing risk-of-bias assessments. *Res Synth Methods* (2021) 12:55–61. doi: 10.1002/jrsm.1411

26. Cossarizza A, Chang H, Radbruch A, Abrignani S, Addo R, Akdis M, Andrä I, Andreata F, Annunziato F, Arranz E, et al. Guidelines for the use of flow cytometry and cell sorting in immunological studies (third edition). *Eur J Immunol* (2021) 51:2708–3145. doi: 10.1002/eji.202170126

27. Boström M, Eriksson Y, Danial J, Björk-Eriksson T, Kalm M. Chronic disturbance in the thalamus following cranial irradiation to the developing mouse brain. *Sci Rep* (2019) 9:9588. doi: 10.1038/s41598-019-45973-8

28. Yamasaki T, Suzuki A, Hasebe R, Horiuchi M. Flow Cytometric Detection of PrP^{Sc} in Neurons and Glial Cells from Prion-Infected Mouse Brains. *J Virol* (2018) 92: doi: 10.1128/JVI.01457-17

29. Williams GP, Schonhoff AM, Jurkuvenaite A, Gallups NJ, Standaert DG, Harms AS. CD4 T cells mediate brain inflammation and neurodegeneration in a mouse model of Parkinson's disease. *Brain* (2021) 144:2047–2059. doi: 10.1093/brain/awab103

30. Ferretti MT, Merlini M, Späni C, Gericke C, Schweizer N, Enzmann G, Engelhardt B, Kulic L, Suter T, Nitsch RM. T-cell brain infiltration and immature antigen-presenting cells in transgenic models of Alzheimer's disease-like cerebral amyloidosis. *Brain Behav Immun* (2016) 54:211–225. doi: 10.1016/j.bbi.2016.02.009

31. Ito M, Komai K, Mise-Omata S, Iizuka-Koga M, Noguchi Y, Kondo T, Sakai R, Matsuo K, Nakayama T, Yoshie O, et al. Brain regulatory T cells suppress astrogliosis and potentiate neurological recovery. *Nature* (2019) 565:246–250. doi: 10.1038/s41586-018-0824-5

32. Daglas M, Draxler DF, Ho H, McCutcheon F, Galle A, Au AE, Larsson P, Gregory J, Alderuccio F, Sashindranath M, et al. Activated CD8+ T Cells Cause Long-Term Neurological Impairment after Traumatic Brain Injury in Mice. *Cell Rep* (2019) 29:1178-1191.e6. doi: 10.1016/j.celrep.2019.09.046

33. Pasciuto E, Burton OT, Roca CP, Lagou V, Rajan WD, Theys T, Mancuso R, Tito RY, Kouser L, Callaerts-Vegh Z, et al. Microglia Require CD4 T Cells to Complete the Fetal-to-Adult Transition. *Cell* (2020) 182:625-640.e24. doi: 10.1016/j.cell.2020.06.026

34. Herz J, Köster C, Crasmöller M, Abberger H, Hansen W, Felderhoff-Müser U, Bendix I. Peripheral T Cell Depletion by FTY720 Exacerbates Hypoxic-Ischemic Brain Injury in Neonatal Mice. *Front Immunol* (2018) 9: doi: 10.3389/fimmu.2018.01696

35. Chu HX, Kim HA, Lee S, Moore JP, Chan CT, Vinh A, Gelderblom M, Arumugam T V, Broughton BR, Drummond GR, et al. Immune Cell Infiltration in Malignant Middle Cerebral Artery Infarction: Comparison with Transient Cerebral Ischemia. *Journal of Cerebral Blood Flow & Metabolism* (2014) 34:450–459. doi: 10.1038/jcbfm.2013.217

36. Zhou Y, Wang X, Tang D, Li Y, Jiao Y, Gan Y, Hu X, Yang L, Yu W, Stetler RA, et al. IL-2mAb reduces demyelination after focal cerebral ischemia by suppressing $CD8^{+}$ T cells. *CNS Neurosci Ther* (2019) 25:532–543. doi: 10.1111/cns.13084

37. Shaw TN, Stewart-Hutchinson PJ, Strangward P, Dandamudi DB, Coles JA, Villegas-Mendez A, Gallego-Delgado J, van Rooijen N, Zindy E, Rodriguez A, et al. Perivascular Arrest of CD8+ T Cells Is a Signature of Experimental Cerebral Malaria. *PLoS Pathog* (2015) 11:e1005210. doi: 10.1371/journal.ppat.1005210

38. Jurado KA, Yockey LJ, Wong PW, Lee S, Huttner AJ, Iwasaki A. Antiviral CD8 T cells induce Zika-virus-associated paralysis in mice. *Nat Microbiol* (2017) 3:141–147. doi: 10.1038/s41564-017-0060-z

39. Unger MS, Li E, Scharnagl L, Poupardin R, Altendorfer B, Mrowetz H, Hutter-Paier B, Weiger TM, Heneka MT, Attems J, et al. CD8+ T-cells infiltrate Alzheimer's disease brains and regulate neuronal- and synapse-related gene expression in APP-PS1 transgenic mice. *Brain Behav Immun* (2020) 89:67–86. doi: 10.1016/j.bbi.2020.05.070

40. Meng H, Zhao H, Cao X, Hao J, Zhang H, Liu Y, Zhu M, Fan L, Weng L, Qian L, et al. Double-negative T cells remarkably promote neuroinflammation after ischemic stroke. *Proceedings of the National Academy of Sciences* (2019) 116:5558–5563. doi: 10.1073/pnas.1814394116

41. Beckmann L, Obst S, Labusek N, Abberger H, Köster C, Klein-Hitpass L, Schumann S, Kleinschnitz C, Hermann DM, Felderhoff-Müser U, et al. Regulatory T Cells Contribute to Sexual Dimorphism in Neonatal Hypoxic-Ischemic Brain Injury. *Stroke* (2022) 53:381–390. doi: 10.1161/STROKEAHA.121.037537

42. Li W, Luo Y, Xu H, Ma Q, Yao Q. Imbalance between T helper 1 and regulatory T cells plays a detrimental role in experimental Parkinson's disease in mice. *Journal of International Medical Research* (2021) 49:030006052199847. doi: 10.1177/0300060521998471

43. Chen C, Chencheng Z, Cuiying L, Xiaokun G. Plasmacytoid Dendritic Cells Protect Against Middle Cerebral Artery Occlusion Induced Brain Injury by Priming Regulatory T Cells. *Front Cell Neurosci* (2020) 14: doi: 10.3389/fncel.2020.00008

44. Maes W, Verschuere T, Van Hoylandt A, Boon L, Van Gool S. Depletion of Regulatory T Cells in a Mouse Experimental Glioma Model through Anti-CD25 Treatment Results in the Infiltration of Non-Immunosuppressive Myeloid Cells in the Brain. *Clin Dev Immunol* (2013) 2013:1–6. doi: 10.1155/2013/952469

45. Rayasam A, Kijak JA, Kissel L, Choi YH, Kim T, Hsu M, Joshi D, Laaker CJ, Cismaru P, Lindstedt A, et al. CXCL13 expressed on inflamed cerebral blood vessels recruit IL-21 producing TFH cells to damage neurons following stroke. *J Neuroinflammation* (2022) 19:125. doi: 10.1186/s12974-022-02490-2

46. Guo Y, Chen X, Li D, Liu H, Ding Y, Han R, Shi Y, Ma X. PR-957 mediates neuroprotection by inhibiting Th17 differentiation and modulating cytokine production in a mouse model of ischaemic stroke. *Clin Exp Immunol* (2018) 193:194–206. doi: 10.1111/cei.13132

47. Beurel E, Lowell JA, Jope RS. Distinct characteristics of hippocampal pathogenic TH17 cells in a mouse model of depression. *Brain Behav Immun* (2018) 73:180–191. doi: 10.1016/j.bbi.2018.04.012

48. He H, Geng T, Chen P, Wang M, Hu J, Kang L, Song W, Tang H. NK cells promote neutrophil recruitment in the brain during sepsis-induced neuroinflammation. *Sci Rep* (2016) 6:27711. doi: 10.1038/srep27711

49. Jin W-N, Shi K, He W, Sun J-H, Van Kaer L, Shi F-D, Liu Q. Neuroblast senescence in the aged brain augments natural killer cell cytotoxicity leading to impaired neurogenesis and cognition. *Nat Neurosci* (2021) 24:61–73. doi: 10.1038/s41593-020-00745-w

50. Zhang Y, Fung ITH, Sankar P, Chen X, Robison LS, Ye L, D'Souza SS, Salinero AE, Kuentzel ML, Chittur S V., et al. Depletion of NK Cells Improves Cognitive Function in the Alzheimer Disease Mouse Model. *The Journal of Immunology* (2020) 205:502–510. doi: 10.4049/jimmunol.2000037

51. Li Z, Li M, Shi SX, Yao N, Cheng X, Guo A, Zhu Z, Zhang X, Liu Q. Brain transforms natural killer cells that exacerbate brain edema after intracerebral hemorrhage. *Journal of Experimental Medicine* (2020) 217: doi: 10.1084/jem.20200213

52. D'Alessandro G, Antonangeli F, Marrocco F, Porzia A, Lauro C, Santoni A, Limatola C. Gut microbiota alterations affect glioma growth and innate immune cells involved in tumor immunosurveillance in mice. *Eur J Immunol* (2020) 50:705–711. doi: 10.1002/eji.201948354

53. Earls RH, Menees KB, Chung J, Gutekunst C-A, Lee HJ, Hazim MG, Rada B, Wood LB, Lee J-K. NK cells clear α-synuclein and the depletion of NK cells exacerbates synuclein pathology in a mouse model of α-synucleinopathy. *Proceedings of the National Academy of Sciences* (2020) 117:1762–1771. doi: 10.1073/pnas.1909110117

54. Dando SJ, Naranjo Golborne C, Chinnery HR, Ruitenberg MJ, McMenamin PG. A case of mistaken identity: CD11c-eYFP $^{+}$ cells in the normal mouse brain parenchyma and neural retina display the phenotype of microglia, not dendritic cells. *Glia* (2016) 64:1331–1349. doi: 10.1002/glia.23005

55. Clarkson BD, Walker A, Harris MG, Rayasam A, Hsu M, Sandor M, Fabry Z. CCR7 deficient inflammatory Dendritic Cells are retained in the Central Nervous System. *Sci Rep* (2017) 7:42856. doi: 10.1038/srep42856

56. Gelderblom M, Gallizioli M, Ludewig P, Thom V, Arunachalam P, Rissiek B, Bernreuther C, Glatzel M, Korn T, Arumugam TV, et al. IL-23 (Interleukin-23)–Producing Conventional Dendritic Cells Control the Detrimental IL-17 (Interleukin-17) Response in Stroke. *Stroke* (2018) 49:155–164. doi: 10.1161/STROKEAHA.117.019101

57. Göbel K, Pankratz S, Asaridou C-M, Herrmann AM, Bittner S, Merker M, Ruck T, Glumm S, Langhauser F, Kraft P, et al. Blood coagulation factor XII drives adaptive

immunity during neuroinflammation via CD87-mediated modulation of dendritic cells. *Nat Commun* (2016) 7:11626. doi: 10.1038/ncomms11626

58. Brioschi S, Wang W-L, Peng V, Wang M, Shchukina I, Greenberg ZJ, Bando JK, Jaeger N, Czepielewski RS, Swain A, et al. Heterogeneity of meningeal B cells reveals a lymphopoietic niche at the CNS borders. *Science (1979)* (2021) 373: doi: 10.1126/science.abf9277

59. Pierson ER, Stromnes IM, Goverman JM. B Cells Promote Induction of Experimental Autoimmune Encephalomyelitis by Facilitating Reactivation of T Cells in the Central Nervous System. *The Journal of Immunology* (2014) 192:929–939. doi: 10.4049/jimmunol.1302171

60. Korin B, Ben-Shaanan TL, Schiller M, Dubovik T, Azulay-Debby H, Boshnak NT, Koren T, Rolls A. High-dimensional, single-cell characterization of the brain's immune compartment. *Nat Neurosci* (2017) 20:1300–1309. doi: 10.1038/nn.4610

61. Liu C, Yang J, Zhang C, Geng X, Zhao H. Remote ischemic conditioning reduced cerebral ischemic injury by modulating inflammatory responses and ERK activity in type 2 diabetic mice. *Neurochem Int* (2020) 135:104690. doi: 10.1016/j.neuint.2020.104690

62. Mracsko E, Javidi E, Na S-Y, Kahn A, Liesz A, Veltkamp R. Leukocyte Invasion of the Brain After Experimental Intracerebral Hemorrhage in Mice. *Stroke* (2014) 45:2107–2114. doi: 10.1161/STROKEAHA.114.005801

63. Trahanas DM, Cuda CM, Perlman H, Schwulst SJ. Differential Activation of Infiltrating Monocyte-Derived Cells After Mild and Severe Traumatic Brain Injury. *Shock* (2015) 43:255–260. doi: 10.1097/SHK.0000000000000291

64. Miró-Mur F, Pérez-de-Puig I, Ferrer-Ferrer M, Urra X, Justicia C, Chamorro A, Planas AM. Immature monocytes recruited to the ischemic mouse brain differentiate into macrophages with features of alternative activation. *Brain Behav Immun* (2016) 53:18–33. doi: 10.1016/j.bbi.2015.08.010

65. Ritzel RM, Patel AR, Grenier JM, Crapser J, Verma R, Jellison ER, McCullough LD. Functional differences between microglia and monocytes after ischemic stroke. *J Neuroinflammation* (2015) 12:106. doi: 10.1186/s12974-015-0329-1

66. Cazareth J, Guyon A, Heurteaux C, Chabry J, Petit-Paitel A. Molecular and cellular neuroinflammatory status of mouse brain after systemic lipopolysaccharide challenge: importance of CCR2/CCL2 signaling. *J Neuroinflammation* (2014) 11:132. doi: 10.1186/1742-2094-11-132

67. Chu HX, Broughton BRS, Ah Kim H, Lee S, Drummond GR, Sobey CG. Evidence That Ly6C ^{hi} Monocytes Are Protective in Acute Ischemic Stroke by Promoting M2 Macrophage Polarization. *Stroke* (2015) 46:1929–1937. doi: 10.1161/STROKEAHA.115.009426

68. Peralta Ramos JM, Iribarren P, Bousset L, Melki R, Baekelandt V, Van der Perren A. Peripheral Inflammation Regulates CNS Immune Surveillance Through the Recruitment of Inflammatory Monocytes Upon Systemic α-Synuclein Administration. *Front Immunol* (2019) 10: doi: 10.3389/fimmu.2019.00080

69. Li Q, Lan X, Han X, Wang J. Expression of Tmem119/Sall1 and Ccr2/CD69 in FACS-Sorted Microglia- and Monocyte/Macrophage-Enriched Cell Populations After Intracerebral Hemorrhage. *Front Cell Neurosci* (2019) 12: doi: 10.3389/fncel.2018.00520

70. Hsieh CL, Kim CC, Ryba BE, Niemi EC, Bando JK, Locksley RM, Liu J, Nakamura MC, Seaman WE. Traumatic brain injury induces macrophage subsets in the brain. *Eur J Immunol* (2013) 43:2010–2022. doi: 10.1002/eji.201243084

71. Hsieh CL, Niemi EC, Wang SH, Lee CC, Bingham D, Zhang J, Cozen ML, Charo I, Huang EJ, Liu J, et al. CCR2 Deficiency Impairs Macrophage Infiltration and Improves Cognitive Function after Traumatic Brain Injury. *J Neurotrauma* (2014) 31:1677–1688. doi: 10.1089/neu.2013.3252

72. DePaula-Silva AB, Gorbea C, Doty DJ, Libbey JE, Sanchez JMS, Hanak TJ, Cazalla D, Fujinami RS. Differential transcriptional profiles identify microglial- and macrophage-specific gene markers expressed during virus-induced neuroinflammation. *J Neuroinflammation* (2019) 16:152. doi: 10.1186/s12974-019-1545-x

73. Lehmann ML, Cooper HA, Maric D, Herkenham M. Social defeat induces depressive-like states and microglial activation without involvement of peripheral macrophages. *J Neuroinflammation* (2016) 13:224. doi: 10.1186/s12974-016-0672-x

74. Cai W, Liu S, Hu M, Sun X, Qiu W, Zheng S, Hu X, Lu Z. Post-stroke DHA Treatment Protects Against Acute Ischemic Brain Injury by Skewing Macrophage Polarity Toward the M2 Phenotype. *Transl Stroke Res* (2018) 9:669–680. doi: 10.1007/s12975-018-0662-7

75. Martin E, El-Behi M, Fontaine B, Delarasse C. Analysis of Microglia and Monocyte-derived Macrophages from the Central Nervous System by Flow Cytometry. *Journal of Visualized Experiments* (2017) doi: 10.3791/55781

76. Honarpisheh P, Lee J, Banerjee A, Blasco-Conesa MP, Honarpisheh P, d'Aigle J, Mamun AA, Ritzel RM, Chauhan A, Ganesh BP, et al. Potential caveats of putative microglia-specific markers for assessment of age-related cerebrovascular neuroinflammation. *J Neuroinflammation* (2020) 17:366. doi: 10.1186/s12974-020-02019-5

77. Nirwane A, Yao Y. SMAlow/undetectable pericytes differentiate into microglia- and macrophage-like cells in ischemic brain. *Cellular and Molecular Life Sciences* (2022) 79:264. doi: 10.1007/s00018-022-04322-1

78. Spiteri AG, Terry RL, Wishart CL, Ashhurst TM, Campbell IL, Hofer MJ, King NJC. High-parameter cytometry unmasks microglial cell spatio-temporal response kinetics in

severe neuroinflammatory disease. *J Neuroinflammation* (2021) 18:166. doi: 10.1186/s12974-021-02214-y

79. Mattei D, Ivanov A, van Oostrum M, Pantelyushin S, Richetto J, Mueller F, Beffinger M, Schellhammer L, vom Berg J, Wollscheid B, et al. Enzymatic Dissociation Induces Transcriptional and Proteotype Bias in Brain Cell Populations. *Int J Mol Sci* (2020) 21:7944. doi: 10.3390/ijms21217944

80. Herron S, Delpech J-C, Madore C, Ikezu T. Using mechanical homogenization to isolate microglia from mouse brain tissue to preserve transcriptomic integrity. *STAR Protoc* (2022) 3:101670. doi: 10.1016/j.xpro.2022.101670

81. Calvo B, Rubio F, Fernández M, Tranque P. Dissociation of neonatal and adult mice brain for simultaneous analysis of microglia, astrocytes and infiltrating lymphocytes by flow cytometry. *IBRO Rep* (2020) 8:36–47. doi: 10.1016/j.ibror.2019.12.004

82. Herzenberg LA, Tung J, Moore WA, Herzenberg LA, Parks DR. Interpreting flow cytometry data: a guide for the perplexed. *Nat Immunol* (2006) 7:681–685. doi: 10.1038/ni0706-681

83. Drucker AM, Fleming P, Chan A-W. Research Techniques Made Simple: Assessing Risk of Bias in Systematic Reviews. *Journal of Investigative Dermatology* (2016) 136:e109–e114. doi: 10.1016/j.jid.2016.08.021

84. Colonna M. TREMs in the immune system and beyond. *Nat Rev Immunol* (2003) 3:445–453. doi: 10.1038/nri1106

85. Keating CE, Houser MC, MacPherson KP, Herrick MK, Coomes A, Joers VL, Oliver D, Johnson AG, Chang J, McEachin Z, et al. Loss of progranulin leads to dysregulation of innate and adaptive immune cell populations, increased susceptibility to experimental colitis, and brain infiltration of peripheral immune cells. *Alzheimer's & Dementia* (2020) 16: doi: 10.1002/alz.042177

86. Rhinn H, Tatton N, McCaughey S, Kurnellas M, Rosenthal A. Progranulin as a therapeutic target in neurodegenerative diseases. *Trends Pharmacol Sci* (2022) 43:641–652. doi: 10.1016/j.tips.2021.11.015

87. Wallings RL, Tansey MG. LRRK2 regulation of immune-pathways and inflammatory disease. *Biochem Soc Trans* (2019) 47:1581–1595. doi: 10.1042/BST20180463

88. Golomb SM, Guldner IH, Zhao A, Wang Q, Palakurthi B, Aleksandrovic EA, Lopez JA, Lee SW, Yang K, Zhang S. Multi-modal Single-Cell Analysis Reveals Brain Immune Landscape Plasticity during Aging and Gut Microbiota Dysbiosis. *Cell Rep* (2020) 33:108438. doi: 10.1016/j.celrep.2020.108438

89. Kovacs EJ, Palmer JL, Fortin CF, Fülöp T, Goldstein DR, Linton P-J. Aging and innate immunity in the mouse: impact of intrinsic and extrinsic factors. *Trends Immunol* (2009) 30:319–324. doi: 10.1016/j.it.2009.03.012

90. Zhang X, Pearsall VM, Carver CM, Atkinson EJ, Clarkson BDS, Grund EM, Baez-Faria M, Pavelko KD, Kachergus JM, White TA, et al. Rejuvenation of the aged brain immune cell landscape in mice through p16-positive senescent cell clearance. *Nat Commun* (2022) 13:5671. doi: 10.1038/s41467-022-33226-8

91. Erickson M, Banks W. Age-Associated Changes in the Immune System and Blood–Brain Barrier Functions. *Int J Mol Sci* (2019) 20:1632. doi: 10.3390/ijms20071632

92. Cumba Garcia LM, Huseby Kelcher AM, Malo CS, Johnson AJ. Superior isolation of antigen-specific brain infiltrating T cells using manual homogenization technique. *J Immunol Methods* (2016) 439:23–28. doi: 10.1016/j.jim.2016.09.002

93. Srakočić S, Josić P, Trifunović S, Gajović S, Grčević D, Glasnović A. Proposed practical protocol for flow cytometry analysis of microglia from the healthy adult mouse brain: Systematic review and isolation methods' evaluation. *Front Cell Neurosci* (2022) 16: doi: 10.3389/fncel.2022.1017976

94. Molina Estevez FJ, Mathews TD, Biffi A, Peviani M. Simultaneous Flow Cytometric Characterization of Multiple Cell Types Retrieved from Mouse Brain/Spinal Cord Through Different Homogenization Methods. *Journal of Visualized Experiments* (2019) doi: 10.3791/60335

95. Kalina T. Reproducibility of Flow Cytometry Through Standardization: Opportunities and Challenges. *Cytometry Part A* (2020) 97:137–147. doi: 10.1002/cyto.a.23901

96. Parks DR, Moore WA, Brinkman RR, Chen Y, Condello D, El Khettabi F, Nolan JP, Perfetto SP, Redelman D, Spidlen J, et al. Methodology for evaluating and comparing flow cytometers: A multisite study of 23 instruments. *Cytometry Part A* (2018) 93:1087–1091. doi: 10.1002/cyto.a.23605

97. Lee JA, Spidlen J, Boyce K, Cai J, Crosbie N, Dalphin M, Furlong J, Gasparetto M, Goldberg M, Goralczyk EM, et al. MIFlowCyt: The minimum information about a flow cytometry experiment. *Cytometry Part A* (2008) 73A:926–930. doi: 10.1002/cyto.a.20623

98. Zhang Z, Ma Z, Zou W, Guo H, Liu M, Ma Y, Zhang L. The Appropriate Marker for Astrocytes: Comparing the Distribution and Expression of Three Astrocytic Markers in Different Mouse Cerebral Regions. *Biomed Res Int* (2019) 2019:1–15. doi: 10.1155/2019/9605265

99. Guttenplan KA, Liddelow SA. Astrocytes and microglia: Models and tools. *Journal of Experimental Medicine* (2019) 216:71–83. doi: 10.1084/jem.20180200

100. Donato R, Sorci G, Riuzzi F, Arcuri C, Bianchi R, Brozzi F, Tubaro C, Giambanco I. S100B's double life: Intracellular regulator and extracellular signal. *Biochimica et Biophysica Acta (BBA) - Molecular Cell Research* (2009) 1793:1008–1022. doi: 10.1016/j.bbamcr.2008.11.009

101. Raponi E, Agenes F, Delphin C, Assard N, Baudier J, Legraverend C, Deloulme J-C. S100B expression defines a state in which GFAP-expressing cells lose their neural stem cell potential and acquire a more mature developmental stage. *Glia* (2007) 55:165–177. doi: 10.1002/glia.20445

102. Ruan C, Elyaman W. A New Understanding of TMEM119 as a Marker of Microglia. *Front Cell Neurosci* (2022) 16: doi: 10.3389/fncel.2022.902372

103. Young KF, Gardner R, Sariana V, Whitman SA, Bartlett MJ, Falk T, Morrison HW. Can quantifying morphology and TMEM119 expression distinguish between microglia and infiltrating macrophages after ischemic stroke and reperfusion in male and female mice? *J Neuroinflammation* (2021) 18:58. doi: 10.1186/s12974-021-02105-2

104. Jurga AM, Paleczna M, Kuter KZ. Overview of General and Discriminating Markers of Differential Microglia Phenotypes. *Front Cell Neurosci* (2020) 14: doi: 10.3389/fncel.2020.00198

105. Hopperton KE, Mohammad D, Trépanier MO, Giuliano V, Bazinet RP. Markers of microglia in post-mortem brain samples from patients with Alzheimer's disease: a systematic review. *Mol Psychiatry* (2018) 23:177–198. doi: 10.1038/mp.2017.246

106. Fransen NL, Hsiao C-C, van der Poel M, Engelenburg HJ, Verdaasdonk K, Vincenten MCJ, Remmerswaal EBM, Kuhlmann T, Mason MRJ, Hamann J, et al. Tissue-resident memory T cells invade the brain parenchyma in multiple sclerosis white matter lesions. *Brain* (2020) 143:1714–1730. doi: 10.1093/brain/awaa117

107. Steinbach K, Vincenti I, Kreutzfeldt M, Page N, Muschaweckh A, Wagner I, Drexler I, Pinschewer D, Korn T, Merkler D. Brain-resident memory T cells represent an autonomous cytotoxic barrier to viral infection. *Journal of Experimental Medicine* (2016) 213:1571–1587. doi: 10.1084/jem.20151916

108. Prasad S, Lokensgard JR. Brain-Resident T Cells Following Viral Infection. *Viral Immunol* (2019) 32:48–54. doi: 10.1089/vim.2018.0084

109. Sedgwick AJ, Ghazanfari N, Constantinescu P, Mantamadiotis T, Barrow AD. The Role of NK Cells and Innate Lymphoid Cells in Brain Cancer. *Front Immunol* (2020) 11: doi: 10.3389/fimmu.2020.01549

110. Cuapio A, Ljunggren H-G. Activated Natural Killer Cells Hit Neurogenesis in the Aging Brain. *Neurosci Bull* (2021) 37:1072–1074. doi: 10.1007/s12264-021-00654-3

111. Earls RH, Lee JK. The role of natural killer cells in Parkinson's disease. *Exp Mol Med* (2020) 52:1517–1525. doi: 10.1038/S12276-020-00505-7

112. Sakata-Kaneko S, Wakatsuki Y, Matsunaga Y, Usui T, Kita T. Altered Th1/Th2 commitment in human CD4+ T cells with ageing. *Clin Exp Immunol* (2001) 120:267–273. doi: 10.1046/j.1365-2249.2000.01224.x

113. D'Agostino PM, Gottfried-Blackmore A, Anandasabapathy N, Bulloch K. Brain dendritic cells: biology and pathology. *Acta Neuropathol* (2012) 124:599–614. doi: 10.1007/s00401-012-1018-0

114. Constant O, Maarifi G, Blanchet FP, Van de Perre P, Simonin Y, Salinas S. Role of Dendritic Cells in Viral Brain Infections. *Front Immunol* (2022) 13: doi: 10.3389/fimmu.2022.862053

115. Ludewig P, Gallizioli M, Urra X, Behr S, Brait VH, Gelderblom M, Magnus T, Planas AM. Dendritic cells in brain diseases. *Biochimica et Biophysica Acta (BBA) - Molecular Basis of Disease* (2016) 1862:352–367. doi: 10.1016/j.bbadis.2015.11.003

116. Clark J, McFarlane C, Cleo G, Ishikawa Ramos C, Marshall S. The Impact of Systematic Review Automation Tools on Methodological Quality and Time Taken to Complete Systematic Review Tasks: Case Study. *JMIR Med Educ* (2021) 7:e24418. doi: 10.2196/24418

117. Marshall IJ, Wallace BC. Toward systematic review automation: a practical guide to using machine learning tools in research synthesis. *Syst Rev* (2019) 8:163. doi: 10.1186/s13643-019-1074-9